

Utah State University

DigitalCommons@USU

Reports

Utah Water Research Laboratory

1-1-1967

Design and Calibration of Submerged Open Channel Flow Measurement Structures: Part 4 - Weirs

Gaylord V. Skogerboe

M. Leon Hyatt

Lloyd H. Austin

Follow this and additional works at: https://digitalcommons.usu.edu/water_rep



Part of the [Civil and Environmental Engineering Commons](#), and the [Water Resource Management Commons](#)

Recommended Citation

Skogerboe, Gaylord V.; Hyatt, M. Leon; and Austin, Lloyd H., "Design and Calibration of Submerged Open Channel Flow Measurement Structures: Part 4 - Weirs" (1967). *Reports*. Paper 80.

https://digitalcommons.usu.edu/water_rep/80

This Report is brought to you for free and open access by the Utah Water Research Laboratory at DigitalCommons@USU. It has been accepted for inclusion in Reports by an authorized administrator of DigitalCommons@USU. For more information, please contact digitalcommons@usu.edu.



Design and Calibration of Submerged
Open Channel Flow Measurement Structures

Part 4

WEIRS

OWRR Project No. B-006-UTAH
Matching Grant Agreement No. 14-01-0001-717
Investigation Period — April 1, 1965 to June 30, 1967

Partial technical completion report prepared for

Office of Water Resources Research
United States Department of the Interior

and

Utah Center for Water Resources Research
Utah State University

Prepared by

Gaylord V. Skogerboe

M. Leon Hyatt

Lloyd H. Austin

Utah Water Research Laboratory
College of Engineering
Utah State University
Logan, Utah

May 1967

Report WG31-5

ABSTRACT

DESIGN AND CALIBRATION OF SUBMERGED OPEN CHANNEL FLOW MEASUREMENT STRUCTURES

PART 4, WEIRS

A number of methods for analyzing submerged (subcritical) flow over weirs has been developed by various investigators. Typical of the approaches applied to this particular problem are those reported by Robinson (1964) and Villemonte (1949). In addition, a method of analyzing submerged flow at open channel constrictions has been developed at Utah State University. All three methods of analysis have been compared by using data collected for various weir shapes. The comparisons showed each method of analysis to be correct, one method complementing each of the other methods. The primary advantage of the techniques developed at Utah State University is that the calibration curves are in reality the rating for any particular structure. The other methods do not yield discharge directly.

Skogerboe, Gaylord V., M. Leon Hyatt, and Lloyd H. Austin. DESIGN AND CALIBRATION OF SUBMERGED OPEN CHANNEL FLOW MEASUREMENT STRUCTURES: PART 4, WEIRS. Research Project Partial Technical Completion Report to Office of Water Resources Research, Department of the Interior, and Utah Center for Water Resources Research. Report WG31-5, Utah Water Research Laboratory, College of Engineering, Utah State University, Logan, Utah. May 1967.

KEYWORDS—flow measurement hydraulics hydraulic structures
*open-channel flow *subcritical flow *submerged flow *weirs.

ACKNOWLEDGMENTS

The existence of this publication is based on support in part from funds provided by the United States Department of the Interior, Office of Water Resources Research, as authorized under the Water Resources Research Act of 1964, Public Law 88-379. The project providing the information used in this report is a part of the program of the Utah Center for Water Resources Research, Utah State University, Logan, Utah. Thanks and appreciation for this support is here acknowledged.

The writers further acknowledge that some of the information used in this report, particularly submerged flow data, was taken from studies by Glen N. Cox, Edwin S. Crump, Carl E. Kindsvater, Herman J. Koloseus, and James R. Villemonte. The writers are particularly grateful to Dr. Villemonte for furnishing his original data.

The cooperation and services of the Utah Water Research Laboratory were invaluable in the publication of this report. Thanks are extended to Miss Donna Higgins for editing this manuscript.

Gaylord V. Skogerboe
M. Leon Hyatt
Lloyd H. Austin

TABLE OF CONTENTS

	Page
Introduction -----	1
Definition of Flow Regimes -----	1
Concepts of Submerged Flow and Free Flow -----	1
Momentum Theory Applied to Weirs -----	3
Simplified Analysis -----	5
General Analysis -----	5
Characteristics of Submerged Flow Over Weirs -----	6
Equation Characteristics -----	6
Submerged Flow Analysis Used by Robinson -----	8
Villemonthe's Submerged Flow Analysis -----	9
Three-dimensional Submerged Flow Analysis -----	11
Comparisons Between Methods of Analysis -----	18
Nappe Condition -----	18
Weir Types Investigated -----	24
Suppressed Sharp-crested -----	25
Contracted Sharp-crested -----	27
Suppressed Ogee Crest -----	27
Crump Weir -----	29
Other Weir Types -----	30
Summary -----	38
References -----	38

LIST OF FIGURES

Figure	Page
1 Control volume for analysis of broad-crested weirs -----	3
2 Simplified control volume for analysis of broad-crested weirs -----	4
3 Relationship between $f(S)$, $\phi_m(S)$, and P/h for broad-crested weirs	7
4 Basic highway embankment model studied by Kindsvater -----	9
5 Two-dimensional submerged flow plot of highway embankment model data -----	10
6 Five-foot suppressed sharp-crested weir -----	11
7 Two-dimensional submerged flow plot of 5-foot suppressed sharp- crested weir data -----	12
8 Submerged flow plot of highway embankment model data as proposed by Villemonte -----	13
9 Submerged flow plot of 5-foot suppressed sharp-crested weir data as proposed by Villemonte -----	14
10 Three-dimensional plot of submerged flow data for highway em- bankment model -----	15
11 Submerged flow calibration curves for highway embankment model	16
12 Submerged flow calibration curves for 5-foot suppressed sharp- crested weir -----	17
13 Three-foot suppressed sharp-crested weir -----	19
14 Six-inch contracted sharp-crested weir -----	19
15 Comparison of USU's and Villemonte's data for 3-foot suppressed sharp-crested weir -----	20
16 Comparison of USU's and Villemonte's data for 6-inch contracted sharp-crested weir -----	21
17 Submerged flow calibration curves for 3-foot suppressed sharp- crested weir -----	22
18 Submerged flow calibration curves for 6-inch suppressed sharp- crested weir -----	23
19 Three-dimensional plot of submerged flow data for Cox's 2.00 foot high suppressed sharp-crested weir -----	24
20 Three-dimensional plot of submegeed flow data for Cox's 5.93 foot high suppressed sharp-crested weir -----	25
21 Submerged flow calibration curves with data for Villemonte's 2-foot suppressed sharp-crested weir -----	26
22 Typical ogee crest weir studied by Koloseus -----	27
23 Three-dimensional plot of submerged flow data for ogee crest weir studied by Koloseus -----	28
24 Test model of Crump weir -----	30
25 Two-dimensional submerged flow plot of Crump weir data -----	31
26 Submerged flow plot of Crump weir data in manner proposed by Villemonte -----	32
27 Three-dimensional plot of submerged flow data for Crump weir ----	33

28	Submerged flow and free flow calibration curves for Crump weir --	34
29	Submerged flow calibration curves and plotted data for symmetrical proportional weir -----	35
30	Submerged flow calibration curves and plotted data for 90° V-notch weir -----	36
31	Submerged flow calibration curves and plotted data for cusp parabolic weir -----	37

LIST OF TABLES

Table	Page
1 Description of weirs investigated -----	2

NOMENCLATURE

Symbol	Definition
C	coefficient in free flow equation
C ₁	coefficient in numerator of submerged flow equation
C ₂	coefficient in denominator of submerged flow equation
F	force
F ₁	hydrostatic force at section 1
F ₂	hydrostatic force at section 2
F ₃	resultant form resistance of broad-crested weir acting on fluid in horizontal direction
F _d	force of downstream end of broad-crested weir acting on fluid
F _f	boundary frictional force
F _u	force of upstream end of broad-crested weir acting on fluid
F _x	force acting in horizontal direction
g	acceleration due to gravity
h	upstream depth of flow measured from crest elevation
n ₁	exponent in free flow equation and numerator of submerged flow equation
n ₂	exponent in denominator of submerged flow equation
P	height of weir
P+E	height of ogee crest weir
q	actual discharge per foot of length of weir crest
q _o	discharge per foot of length based on upstream depth of flow which has been increased due to submergence
Q	actual total flow rate, or discharge
Q _o	total discharge based on upstream depth of flow which has been increased due to submergence
S	submergence, which is ratio of a downstream depth to an upstream depth with both depths referenced to a common elevation
S _t	transition submergence
t	downstream depth of flow measured from crest elevation
V	average velocity
V ₁	average velocity at section 1
V ₂	average velocity at section 2
y	flow depth
β	momentum correction coefficient
γ	specific weight of fluid
ρ	density of fluid
f(S)	$1/(-\log S)$
φ _m (S)	$1/\sqrt{(1 - (S)^3) / S (1 + S)}$

INTRODUCTION

At Utah State University, considerable effort has been devoted to the analysis of submerged flow at open channel constrictions. A method of analyzing submerged flow was first developed for a trapezoidal flume by Hyatt (1965). Later studies verified the method of analysis for a rectangular flume (Skogerboe, Walker, and Robinson, 1965) and Parshall flumes (Skogerboe, Hyatt, Johnson, and England, 1965). Because of previous findings it was felt this method of analyzing submerged flow could be applied to various types of weirs.

The original development of the parameters and relationships which describe the submerged flow condition came from a combination of dimensional analysis and empiricism. Further verification of the parameters developed in this manner is obtained by employing momentum relationships. Application of momentum theory to broad-crested weirs results in a theoretical equation which describes submerged flow over these weirs and supplements the empirically developed equation.

The efforts of many investigators who have collected both free and submerged flow data for weirs have been extensively used throughout this report. Literature sources were screened for data which typified particular types of weir structures. Data selected from these studies were subjected to the submerged flow analysis developed by the writers and compared with methods proposed by other investigators. Typical of the types of structures analyzed are the suppressed, contracted, sharp-crested, and broad-crested weirs of various sizes and shapes. A complete listing of the weirs studied is found in Table 1.

DEFINITION OF FLOW REGIMES

The two most significant flow regimes or flow conditions are free (critical) flow and submerged (subcritical) flow. The distinguishing difference between the two is that critical depth occurs usually near the crest of the weir for the free flow condition. To determine the free flow discharge, this critical-flow control requires only the measurement of a depth upstream from the point of critical depth. When the downstream or tailwater depth is raised sufficiently, the flow depth at the crest becomes greater than the critical depth, and submerged flow conditions exist. With submerged flow, a change in the tailwater depth also affects the upstream depth and a rating for the weir requires that two flow depths be measured, one upstream and one downstream from the structure. The flow condition at which the regime changes from free flow to submerged flow is a transition state and the value of submergence at which this condition occurs is often referred to as the transition submergence, symbolized by S_t .

CONCEPTS OF SUBMERGED FLOW AND FREE FLOW

Dimensional analysis was first applied to a trapezoidal flume (Hyatt, 1965) to develop the dimensionless parameters describing submerged flow. Manipulation of the equation (Skogerboe, Hyatt, and Eggleston, 1967) relating the dimensionless parameters yields a submerged flow discharge

equation which is dependent upon only the upstream and downstream flow depths. The general form of the submerged flow equation, which is

Table 1. Description of weirs investigated.

Type Weir	Crest Height, P. ft.	Crest Length, ft.	Free Flow Equation cfs	Submerged Flow Equation cfs	Slope of Calibration Curves, n_1	S_t %	Source of Data
Embankment	1.17	----	$q = 3.19 h^{1.53}$	$= \frac{2.41 (h - t)^{1.53}}{(-\log t/h)^{1.20}}$	1.53	85	Kindsvater (1964)
5-foot Suppressed Sharp-crested	2.00	5.00	$Q = 17.65 h^{1.50}$	-----	1.50	0	USU (1967)
3-foot Suppressed Sharp-crested	2.00	3.00	$Q = 10.1 h^{1.50}$	-----	1.50	0	Villemonte (1949) USU (1967)
6-inch Contracted Sharp-crested	1.00	0.50	$Q = 1.48 h^{1.44}$	-----	1.44	0	Villemonte (1949) USU (1967)
2-foot Suppressed Sharp-crested P = 2 feet	2.00	1.96	$Q = 6.85 h^{1.55}$	$= \frac{4.83 (h - t)^{1.55}}{- (\log t/h + 0.0015)}$	1.55	0	Cox (1928)
2-foot Suppressed Sharp-crested P = 5.93 feet	5.93	2.00	$Q = 6.86 h^{1.52}$	$= \frac{4.66 (h - t)^{1.52}}{- (\log t/h + 0.0015)}$	1.52	0	Cox (1928)
Ogee Crest	1.0	----	$q = 4.69 h^{1.69}$	$= \frac{3.44 (h - t)^{1.69}}{[-\log t/h + 0.0025]}^{1.20}$	1.69	50-60	Koloseus (1951)
Crump Weir	0.25	1.67	$Q = 8.33 h^{1.75}$	$= \frac{5.71 (h - t)^{1.75}}{[-\log t/h]^{1.36}}$	1.75	77	Crump (1952)
Symmetrical Proportional	1.00	1.00	$Q = 0.863(h - 0.03)$	-----	1.00	0	Villemonte (1949)
90° V-notch	2.00	2.00	$Q = 2.54 h^{2.51}$	-----	2.50	15-25	Villemonte (1949)
Cusp Parabolic	0.83	0.83	$Q = 0.594 h^{3.32}$	-----	3.32	20-30	Villemonte (1949)

also applicable to weirs, can be expressed as

$$Q = \frac{C_1 (h - t)^{n_1}}{[-(\log t/h + C_2)]^{n_2}} \dots \dots \dots (1)$$

where h and t are flow depths measured upstream and downstream from the structure, C_1 and C_2 are coefficients which depend upon the geometry of the structure, and n_1 and n_2 are exponents which are also related to the structure geometry. The calibration curves depicting this relationship are a family of curves obtained by plotting discharge, Q , as the ordinate, difference between upstream and downstream depths of flow, $h - t$, as the abscissa, and submergence, t/h , as the varying parameter.

The free flow equation for weirs can be expressed by

$$Q = C h^{n_1} \dots \dots \dots (2)$$

It was discovered from the flume studies (Skogerboe, Hyatt, and Eggleston, 1967) and the weir investigations, that the exponent of the $h - t$ term in the submerged flow equation (Eq. 1) is identical to the exponent of h in the free flow equation (Eq. 2) for any given structure.

MOMENTUM THEORY APPLIED TO WEIRS

Application of momentum theory can result in the development of submerged flow discharge equations for weirs, flumes, or other structures. Such equations complement and verify the format of the empirical equations developed from dimensional analysis. A broad-crested weir will be selected to illustrate the application of momentum theory. A control volume of fluid will be used which is bounded by the vertical sections at 1 and 2, the water surface, and the surface of the weir, as shown in Fig 1.

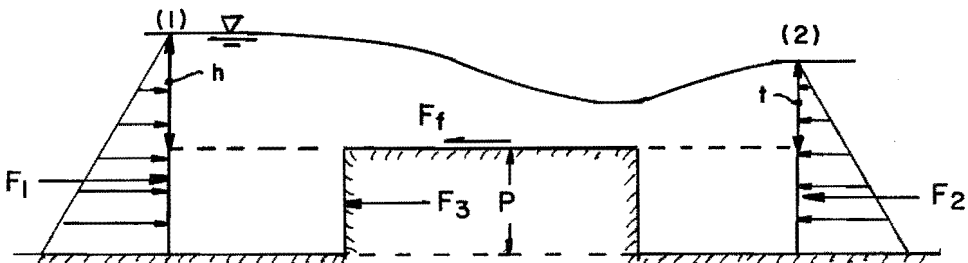


Fig. 1. Control volume for analysis of broad-crested weirs.

The force of the broad-crested weir on the fluid will be designated as F_u for the upstream face and F_d for the downstream face. Assuming the pressure acting on the upstream wall of the weir is hydrostatic and due to the water surface elevation at section 1, while the pressure acting on the downstream wall of the weir is hydrostatic and due to the water surface elevation at section 2, F_u and F_d can be written as

$$F_u = \gamma P (h + P/2) \dots \dots \dots (3)$$

$$F_d = \gamma P (t + P/2) \dots \dots \dots (4)$$

$$\begin{aligned} F_3 &= F_u - F_d \\ &= \gamma P (h + P/2) - \gamma P (t + P/2) \\ &= \gamma P (h - t) \dots \dots \dots (5) \end{aligned}$$

The forces acting on the control volume at section 1 and 2 (Fig. 1) can be determined by assuming hydrostatic pressure distributions.

$$F_1 = \gamma (h + P)^2 / 2 \quad \dots \dots \dots (6)$$

$$F_2 = \gamma (t + P)^2 / 2 \quad \dots \dots \dots (7)$$

If friction losses are neglected ($F_f = 0$), the summation of forces in the horizontal direction can be evaluated.

$$\Sigma F_x = F_1 - F_2 - F_3 \quad \dots \dots \dots (8)$$

$$\begin{aligned} \Sigma F_x &= \gamma (h + P)^2 / 2 - \gamma (t + P)^2 / 2 - \gamma P (h - t) \\ &= \gamma (h^2 - t^2) / 2 \quad \dots \dots \dots (9) \end{aligned}$$

The same equation for the resultant horizontal force (Eq. 9) can be obtained using the simplified control volume shown in Fig. 2.

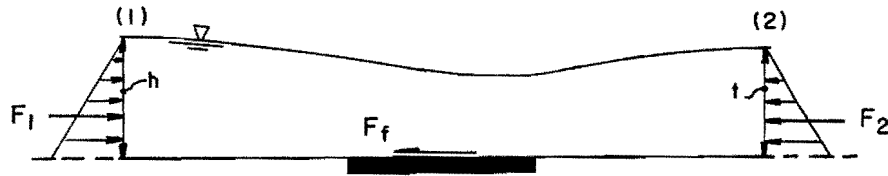


Fig. 2. Simplified control volume for analysis of broad-crested weirs.

Hydrostatic pressure distributions will be assumed at sections 1 and 2.

$$F_1 = \gamma h^2 / 2 \quad \dots \dots \dots (10)$$

$$F_2 = \gamma t^2 / 2 \quad \dots \dots \dots (11)$$

Again, the friction forces will be neglected ($F_f = 0$).

$$\Sigma F = F_1 - F_2 \quad \dots \dots \dots (12)$$

$$\begin{aligned} \Sigma F &= \gamma h^2 / 2 - \gamma t^2 / 2 \\ &= \gamma (h^2 - t^2) / 2 \quad \dots \dots \dots (13) \end{aligned}$$

Since Eqs. 9 and 13 are identical, two methods of analysis are suggested for deriving theoretical submerged flow discharge equations. A simplified analysis can be made using the control volume shown in Fig. 2 and assuming uniform velocity distributions over the flow depths, h and t. A more general submerged flow equation can be derived using the control volume shown in Fig. 1, and assuming uniform velocity distributions over the upstream flow depth, h + P, and the downstream flow depth, t + P. The simplified analysis might be considered appropriate if the flow depths, h and t, are measured at the upstream edge and downstream edge of the weir crest, respectively. The more general analysis requires

that the flow depths, h and t , be measured at a sufficient distance upstream and downstream from the weir crest in order for the assumption of uniform velocity distribution to be valid. Submerged flow equations will be developed for both methods of analysis.

Simplified Analysis

The following analysis is based on the control volume shown in Fig. 2. For the one-dimensional control volume, the momentum equation can be written as

$$\Sigma F = q \rho (\beta_2 V_2 - \beta_1 V_1) \dots \dots \dots (14)$$

By using Eq. 13 for the summation of forces, and assuming uniform velocity distributions at sections 1 and 2

$$\gamma h^2/2 - \gamma t^2/2 = q \rho (V_2 - V_1) \dots \dots \dots (15)$$

The continuity equation, $q = yV$, can be employed if steady flow is assumed.

$$\frac{\gamma h^2}{2} - \frac{\gamma t^2}{2} = \frac{q\gamma}{g} \left[\frac{q}{t} - \frac{q}{h} \right] \dots \dots \dots (16)$$

Solving for the discharge per foot of width, q

$$q = \frac{(g/2)^{1/2}}{\sqrt{\frac{1}{th(h+t)}}} \dots \dots \dots (17)$$

Multiplying numerator and denominator by $(h - t)^{3/2}$

$$q = \frac{(g/2)^{1/2} (h - t)^{3/2}}{\sqrt{\frac{(h - t)^3}{th(h+t)} \frac{h^2}{h^2}}} \dots \dots \dots (18)$$

$$q = \frac{(g/2)^{1/2} (h - t)^{3/2}}{\sqrt{\frac{(1 - t/h)^3}{t/h(1 + t/h)}}} \dots \dots \dots (19)$$

Let the submergence, t/h , be represented by S .

$$q = \frac{(g/2)^{1/2} (h - t)^{3/2}}{\sqrt{\frac{(1 - S)^3}{S(1 + S)}}} \dots \dots \dots (20)$$

General Analysis

The following analysis is made using the control volume shown in Fig. 1. Assuming uniform velocity distributions at sections 1 and 2, the following momentum equation can be written

$$\Sigma F_x = q \rho (V_2 - V_1) \dots \dots \dots (21)$$

The summation of horizontal forces is given by Eq. 9.

$$\gamma (h^2 - t^2)/2 = q \rho (V_2 - V_1) \dots \dots \dots (22)$$

Assuming steady flow, the continuity equation, $q = Vy$, can be employed.

$$q = V_1 (h + P) = V_2 (t + P) \dots \dots \dots (23)$$

The continuity equation can be substituted into Eq. 22.

$$\frac{\gamma (h^2 - t^2)}{2} = q \frac{\gamma}{g} \left[\frac{q}{t + P} - \frac{q}{h + P} \right] \dots \dots (24)$$

Solving for the discharge per foot of weir crest, q

$$q = (g/2)^{1/2} \sqrt{(h + t) (t + P) (h + P)} \dots \dots \dots (25)$$

Multiplying the right hand side by $(h - t)^{3/2} / (h - t)^{3/2}$

$$q = \frac{(g/2)^{1/2} (h - t)^{3/2}}{\sqrt{\frac{(h - t)^3}{(h + t) (t + P) (h + P)}}} \dots \dots \dots (26)$$

Multiplying the numerator and denominator inside the radical by h^3

$$q = \frac{(g/2)^{1/2} (h - t)^{3/2}}{\sqrt{\frac{(1 - t/h)^3 h^3}{(h + t) (t + P) (h + P)}}} \dots \dots \dots (27)$$

Let the submergence, t/h , be designated by S .

$$q = \frac{(g/2)^{1/2} (h - t)^{3/2}}{\sqrt{\frac{(1 - S)^3}{(1 + S) (S + P/h) (1 + P/h)}}} \dots \dots \dots (28)$$

When $P = 0$

$$q = \frac{(g/2)^{1/2} (h - t)^{3/2}}{\sqrt{\frac{(1 - S)^3}{(1 + S) S}}} \dots \dots \dots (29)$$

which is identical to the submerged flow equation developed from the simple analysis (Eq. 20).

CHARACTERISTICS OF SUBMERGED FLOW OVER WEIRS

Equation Characteristics

Although the assumptions made in the development of the theoretical submerged flow equations are not entirely valid, the equations do contain certain characteristics which can be compared with the submerged flow equation developed from dimensional analysis. In order to make a comparison between the two submerged flow equations (Eqs. 1 and 28), assume C_s is equal to zero in Eq. 1. This assumption will later prove to be valid for broad-crested weirs. Define the denominator of Eq. 1 as $1/f(S)$.

$$f(S) = \frac{1}{-\log S} \dots \dots \dots (30)$$

Define the denominator of Eq. 28 as $1/\phi_m(S)$.

$$\phi_m(S) = \frac{1}{\sqrt{\frac{(1 - S)^3}{(1 + S) (S + P/h) (1 + P/h)}}} \dots \dots \dots (31)$$

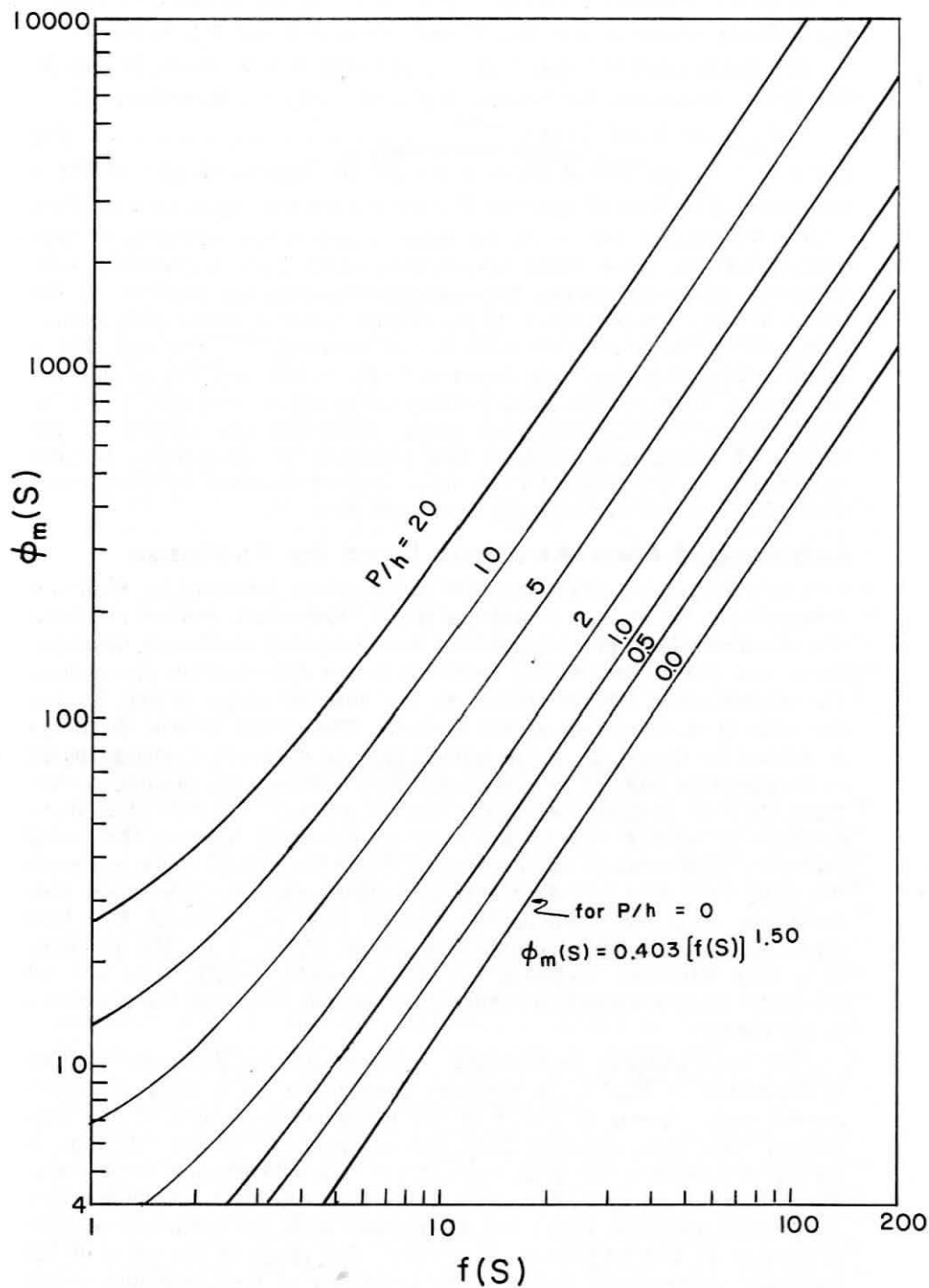


Fig. 3. Relationship between $f(S)$, $\phi_m(S)$, and P/h for broad-crested weirs.

A test of the relationship between $f(S)$ and $\phi_m(S)$ can be made by assigning arbitrary values of S in Eq. 30 and values of S and P/h in Eq. 31.

The comparison between $f(S)$, $\phi_m(S)$, and P/h is shown in Fig. 3. For $P/h = 0$, an equation between $f(S)$ and $\phi_m(S)$ can be written

$$\phi_m(S) = 0.403 [f(S)]^{1.50} \dots \dots \dots (32)$$

For $P/h > 0$, the lines of constant P/h for the logarithmic plot of Fig. 3 are curved. The lines of constant P/h have a constant slope of 1.50 when $f(S) > 10$. When $f(S) = 10$, the submergence is approximately 80 percent. Hence, for those weirs investigated which have a transition submergence value, S_t , greater than 80 percent, only the portions of the curves in Fig. 3 where $f(S) > 10$ are of importance. A relationship similar to Eq. 32 can be written for each line of constant P/h . The fact that a simple relationship does exist between $f(S)$, $\phi_m(S)$, and P/h is of great importance. Such a relationship verifies the correctness of Eqs. 1 and 28, whose formats complement each other, indicating the validity of the method of analyzing submerged flow proposed by the writers. Further verification of this method of analysis can be obtained by comparison with other methods of analyzing submerged flow.

Submerged Flow Analysis Used by Robinson

One approach to submerged flow analysis was presented by Robinson (1964), for a trapezoidal measuring flume. Robinson's method consisted of a two-dimensional plot composed of three variables (discharge, upstream depth, and downstream depth) formed into two dimensionless parameters. The submergence, t/h , is plotted as the abscissa (Figs. 5 and 7) and the ratio Q/Q_0 is plotted as the ordinate. The actual or true discharge is defined by Q and Q_0 is the critical flow or observed discharge based on the upstream depth of flow which has been increased due to submergence. When the ratio of Q/Q_0 reaches the value of 1.0, a critical flow (free flow) condition is reached because the observed discharge becomes the actual discharge. The value of submergence at which the plotted curve intersects the Q/Q_0 ratio of 1.0 is the transition submergence, S_t . Submerged flow conditions exist for submergences greater than S_t , whereas free flow conditions exist for submergences less than S_t ($Q/Q_0 = 1$). The geometry of a weir structure, including its shape, height, length, etc., will all effect the value of transition submergence as well as change the placement of the curve.

The basic highway embankment model studied by Kindsvater (1964) is illustrated in Fig. 4. A highway embankment is a form of broad-crested weir. Shown in Fig. 5 is the two-dimensional plot of the submerged flow data obtained from the embankment model. In Fig. 5, the curve intersects the Q/Q_0 ratio of 1.0 at a submergence value somewhere between 85 and 88 percent. This indicates that submerged flow conditions (transition state) are not reached until the submergence ratio is between 85 and 88 percent, or greater. The range in the value of the transition submergence is due to the instability of transition flow conditions. Usually, the transition submergence is obtained by generating laboratory data in the vicinity of the transition state, or setting the free flow and submerged flow equations equal to one another. The writers feel

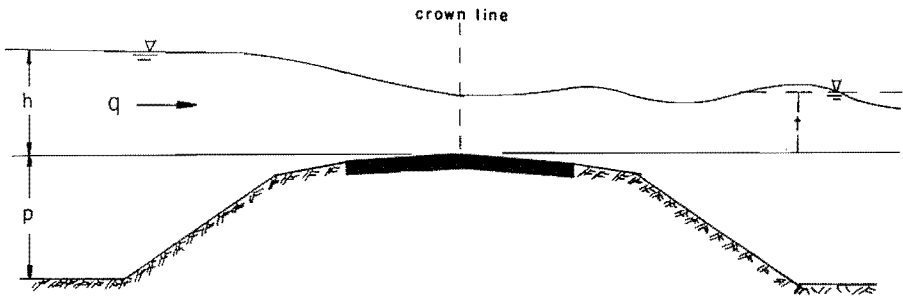


Fig. 4. Basic highway embankment model studied by Kindsvater.

that a finite value of S_1 should exist, although exact determination may be difficult to accomplish.

Further illustration of the submerged flow analysis used by Robinson (1964) can be made utilizing the 5-foot suppressed sharp-crested weir shown in Fig. 6. Data collected from this weir, which was tested at Utah State University, produced the two-dimensional submerged flow curve shown in Fig. 7. For the 5-foot sharp-crested weir, the curve intersects the discharge ratio, Q/Q_0 , at 1.0 when the submergence is zero. Consequently, the transition submergence is zero. Figs. 5 and 7 represent two-dimensional submerged flow plots for two very different types of weirs, as indicated by the placement of the curves. The scatter of the data in Figs. 5 and 7 is typical of most two-dimensional plots. The real problem lies in the correct placement of the curve. In both Figs. 5 and 7, the placement of the curve was obtained by plotting the data in the manner proposed in this report.

Villemonte's Submerged Flow Analysis

Another approach to analyzing submerged flow over weirs is that developed by Villemonte (1949) who considers the discharge in two parts: "(1) a free-fall flow operating under an effective head equal to the difference in upstream and downstream levels, and (2) a submerged orifice likewise operating under a head equal to the difference in upstream and downstream levels." Utilizing Villemonte's development, the data is plotted two-dimensionally with the dimensionless discharge ratio, Q/Q_0 , plotted as the ordinate and $1-S^{n_1}$ plotted as the abscissa, where S is the submergence ratio. The discharge ratio is defined in the same manner as used by Robinson (1964), where free flow conditions exist when Q/Q_0 is equal to 1.0. The transition submergence is the value of S at which the curve intersects the discharge ratio of unity (1.0).

Villemonte's analysis yields a straight line plot on logarithmic paper. For the various types of weirs studied by Villemonte (1949), the subcritical flow curves are drawn through the points (1.0, 1.0) and (0.1, 0.4). For many weir shapes, the data indicates this to be the case, but for other weirs, such is not the case. The discrepancy is acknowledged by Villemonte and dashed lines are drawn to best fit the data for some weir shapes. With different weir structures, one would assume the submergence ratio at which the flow regime changes from critical to subcritical would vary and the curve would intersect the Q/Q_0 ratio of 1.0 at values of submergence different from zero percent ($1-S^{n_1} = 1.0$).

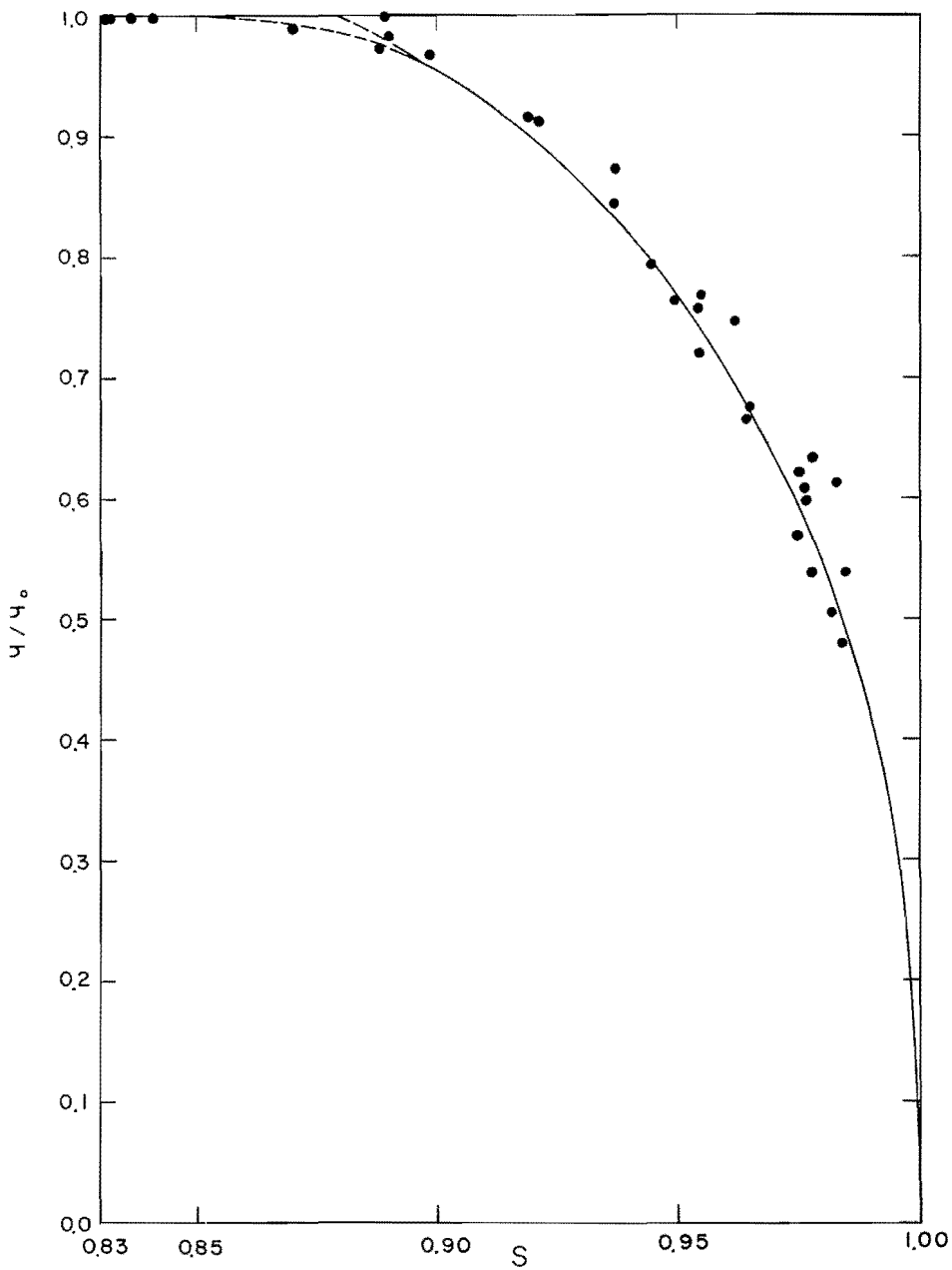


Fig. 5. Two-dimensional submerged flow plot of highway embankment model data.

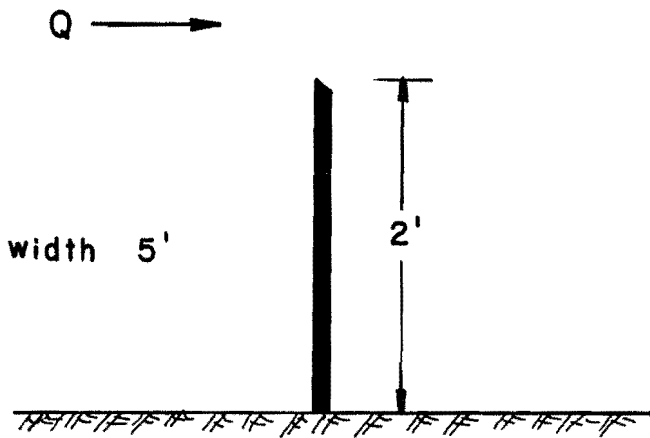


Fig. 6. Five-foot suppressed sharp-crested weir.

The embankment data obtained from the study by Kindsvater (1964) is plotted in Fig. 8 using Villemonte's analysis. The point at which the curve intersects the discharge ratio of unity varies, producing a S_t value somewhere between 85 and 88 percent, as indicated in Fig. 5 where the data was plotted in the manner used by Robinson (1964). However, the curve does have a S_t value somewhere between 85 and 88 percent, and not zero percent. The submerged flow data for the 5-foot sharp-crested weir is plotted in Fig. 9 using the analysis proposed by Villemonte (1949). The plot again produces a straight line, with the curve intersecting the Q/Q_0 ratio of 1.0 at a submergence of zero percent. The same S_t value was obtained for the method used by Robinson (1964) which is plotted in Fig. 7.

Three-Dimensional Submerged Flow Analysis

The method of submerged flow analysis being proposed (Skogerboe, Hyatt, and Eggleston, 1967) is a calibration curve consisting of a family of lines of constant submergence. The calibration curves are obtained by plotting three-dimensionally on logarithmic paper the discharge, Q , as the ordinate, difference between the upstream and downstream depths of flow, $h - t$, as the abscissa, and submergence, t/h , as the varying parameter. Essentially such plots are the graphical presentation of the approximate (Skogerboe, Hyatt, and Eggleston, 1967) submerged flow equation (Eq. 1). Hence, once measurements of h and t are made, the discharge for a given flow condition may be obtained from the calibration curves for that structure by the intersection of the $h - t$ value and the t/h value. Typical of such plots is Fig. 10 in which the embankment data of Kindsvater (1964) is again plotted. The lines of constant submergence which best fit the data are drawn with the slope, n_1 , corresponding to the free flow slope. In Fig. 10, the constant submergence lines of 89.0, 93.7, 95.4, 96.4, 97.5, and 98.5 percent have been drawn at the free flow slope for the embankment, which is 1.53 (Table 1). The equation fitting the format of Eq. 1 which describes the submerged highway embankment model is

$$q = \frac{2.41 (h - t)^{1.53}}{(-\log t/h)^{1.20}} \dots \dots \dots (33)$$

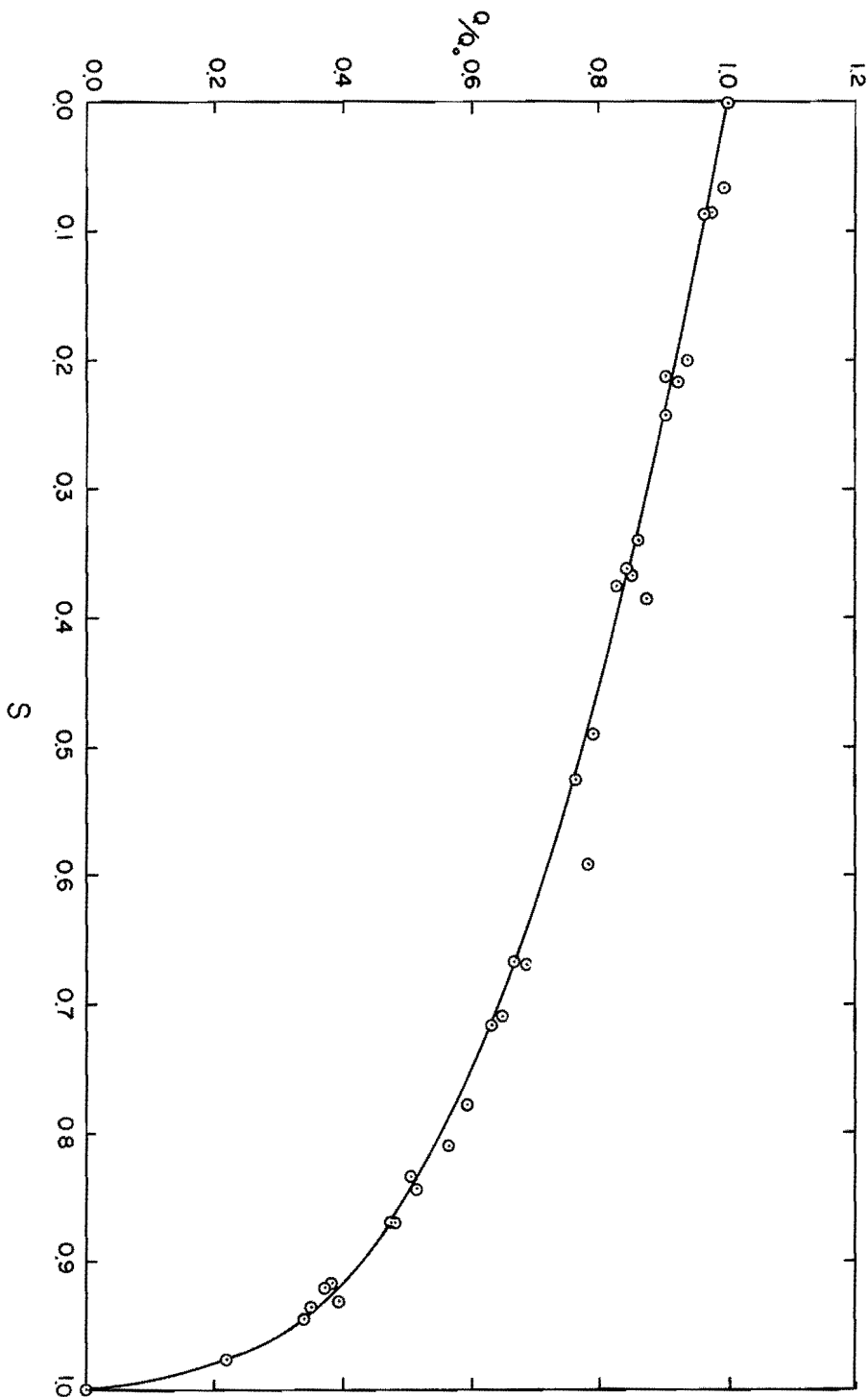


Fig. 7. Two-dimensional submerged flow plot of 5-foot suppressed sharp-crested weir data.

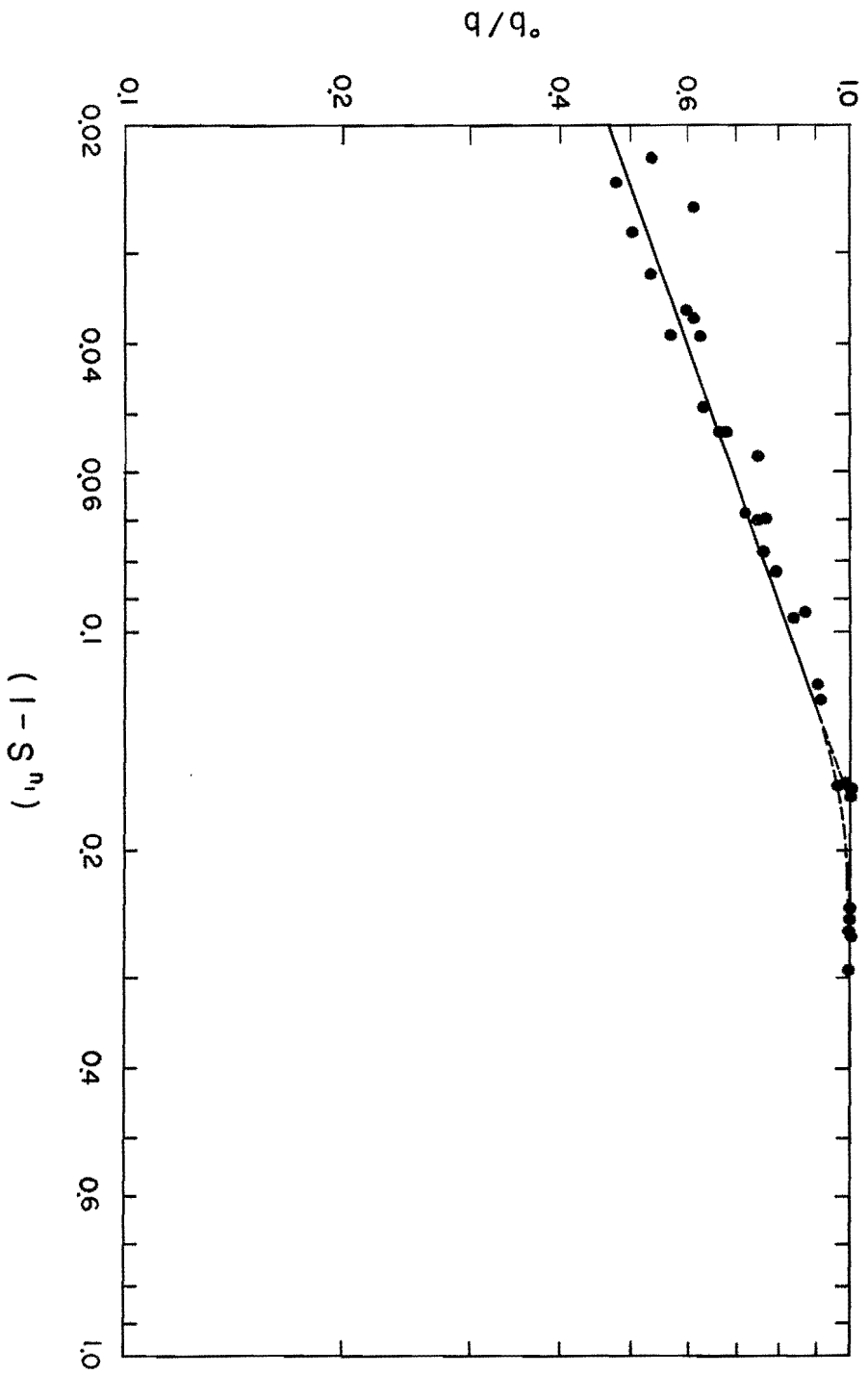


Fig. 8. Submerged flow plot of highway embankment model data as proposed by Villemonte.

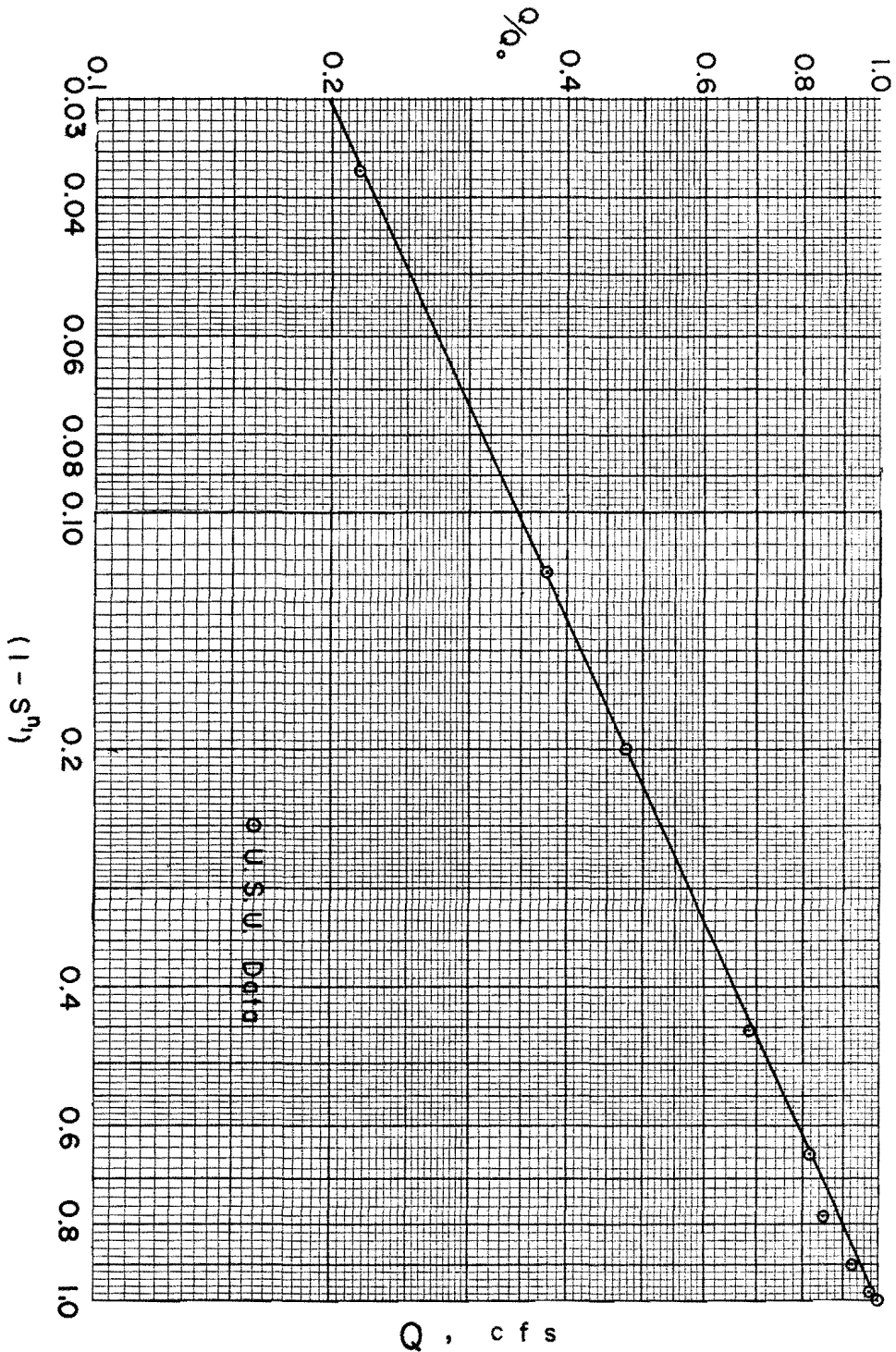


Fig. 9. Submerged flow plot of 5-foot suppressed sharp-crested weir data as proposed by Villemonte.

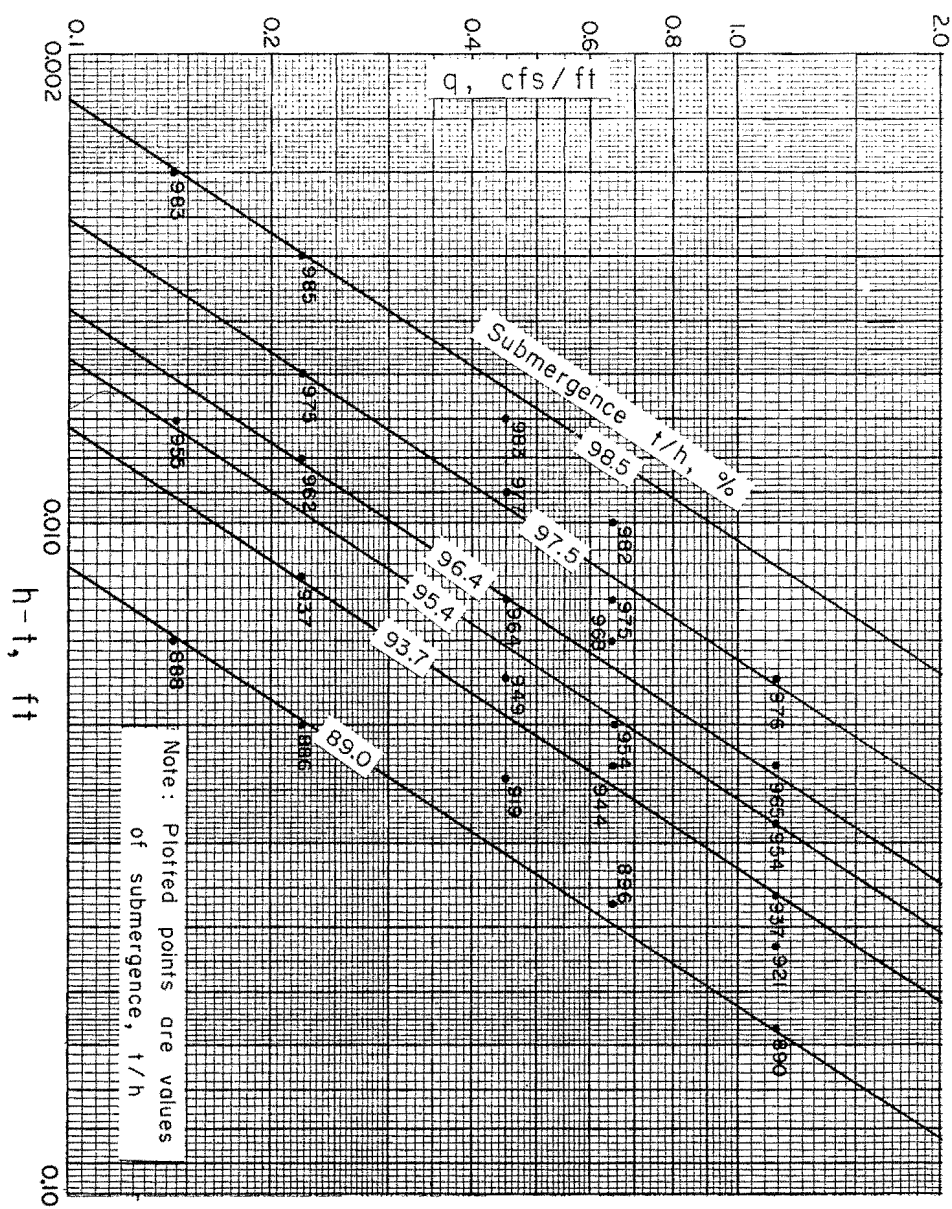


Fig. 10. Three-dimensional plot of submerged flow data for highway embankment model.

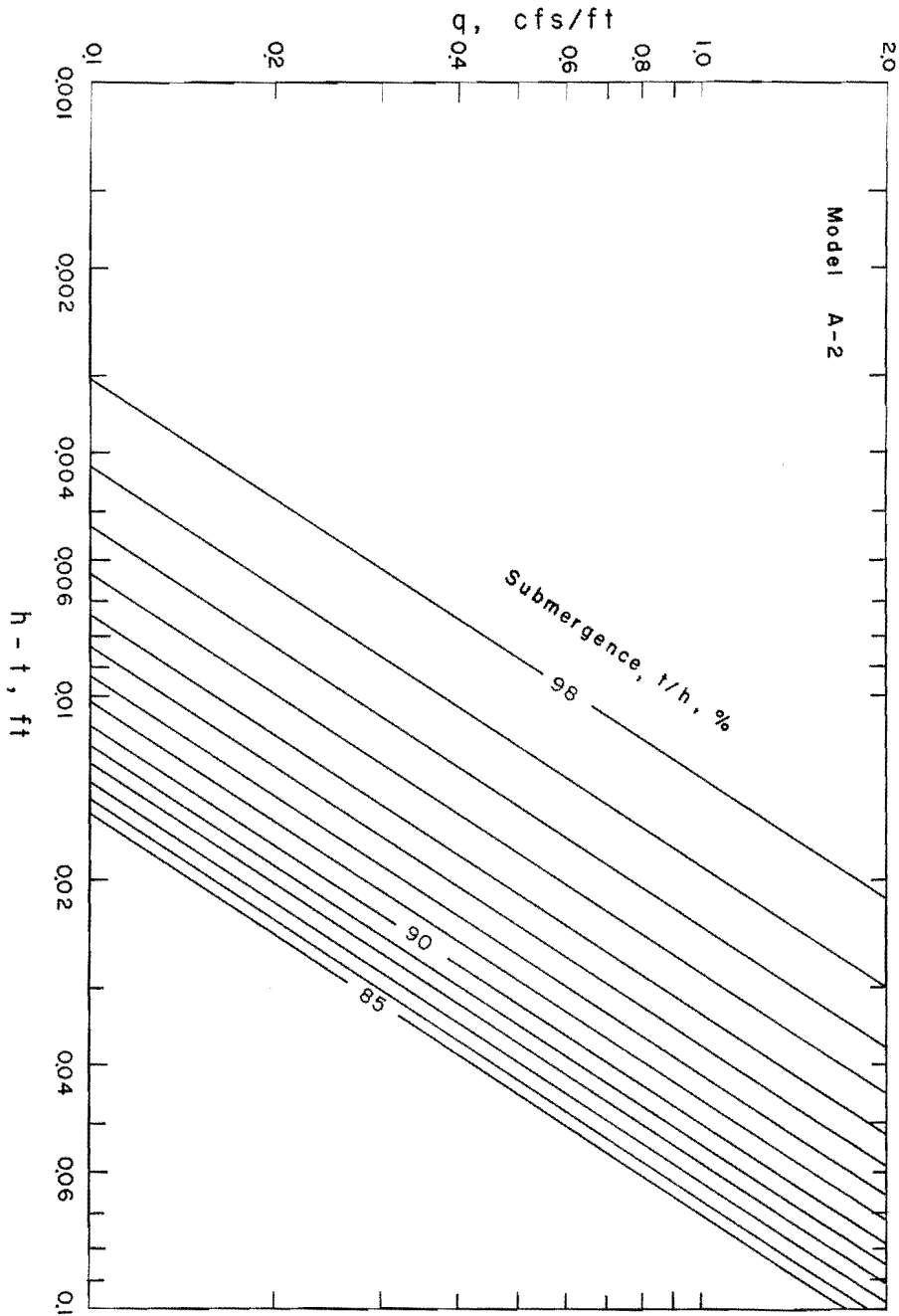


Fig. 11. Submerged flow calibration curves for highway embankment model.

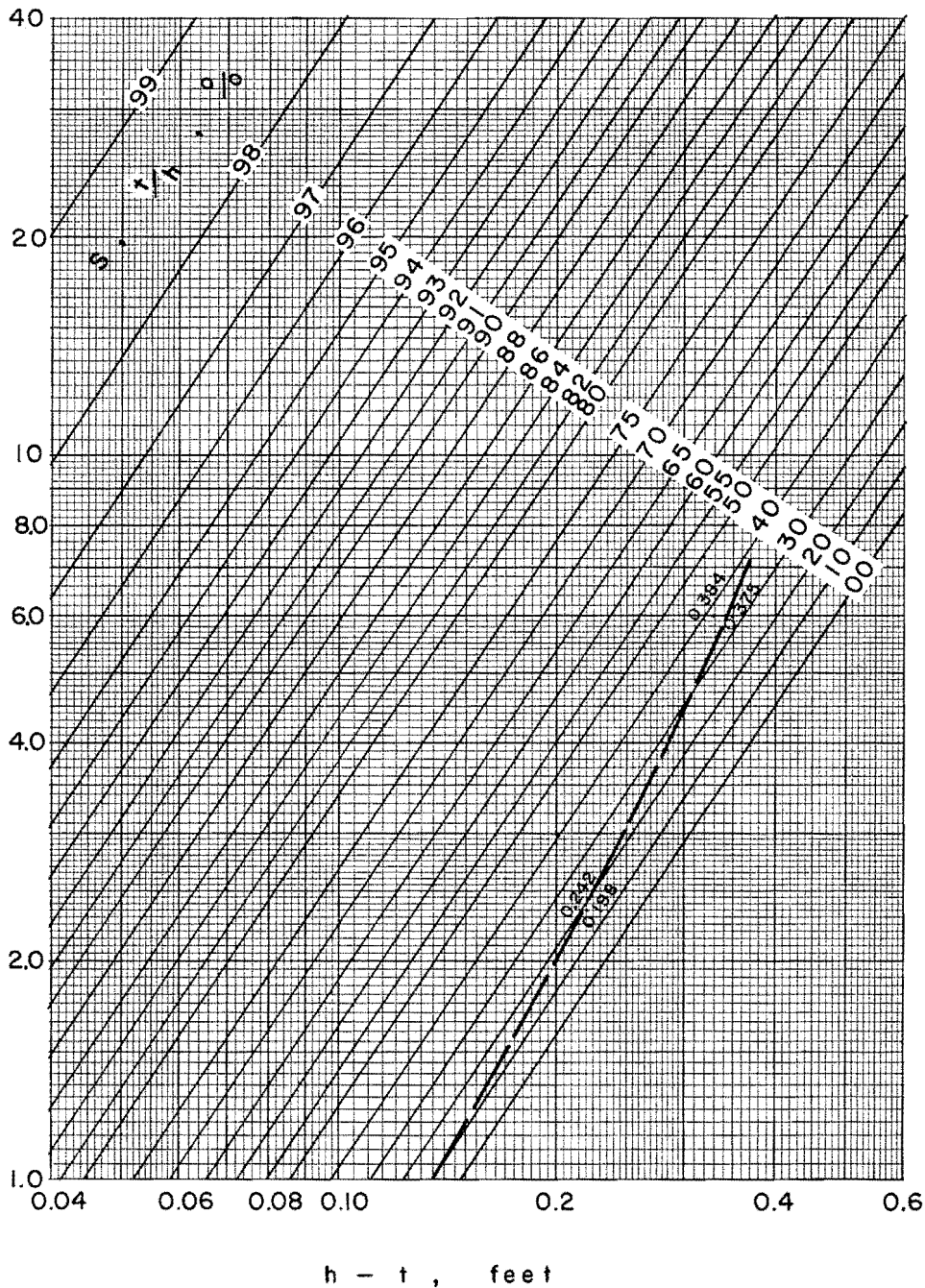


Fig. 12. Submerged flow calibration curves for 5-foot suppressed sharp-crested weir.

This equation describes the submerged flow region from 85 to 98 percent submergence. The complete submerged flow calibration curves for the embankment model are shown in Fig. 11.

For the 5-foot sharp-crested weir no attempt was made to write a subcritical flow equation over the full range of submergence values (0 to 99 percent). However, Fig. 12 is the three-dimensional rating for the 5-foot sharp-crested weir. The slope of the lines of constant submergence is 1.50 (Table 1).

Comparisons Between Methods of Analysis

To obtain uniformity in comparing the two-dimensional plot used by Robinson (1964) and the three-dimensional plot developed at Utah State University, the same data was used in preparing Figs. 5 and 11 and for Figs. 7 and 12. The same results are obtained by using either Figs. 5 or 11, or by using either Figs. 7 or 12, but additional calculations must be made to obtain the discharge when Figs. 5 and 7 are used. The primary difficulty with the two-dimensional plots is accurately determining the location of the curve.

The data from the embankment model and the 5-foot sharp-crested weir are plotted in Figs. 8 and 9, respectively, using the analysis proposed by Villemonte (1949). Although Villemonte's analysis does allow the submerged flow calibration curve to be accurately placed, the discharge is not obtained directly. Instead, additional computations are required.

To further compare the method of analysis proposed by Villemonte (1949) with the three-dimensional analysis developed at Utah State University, some of the weirs studied by Villemonte were also tested in the laboratory by the writers. The weirs selected for additional study were the 3-foot suppressed sharp-crested weir (Fig. 13) and the 6-inch contracted sharp-crested weir (Fig. 14). The geometry of the weirs and channel, along with the locations for measuring the flow depths were identical in both studies. The consistency and compatibility of both sets of data (Villemonte and USU) is indicated by Figs. 15 and 16 which show the data plotted in the manner advocated by Villemonte. For these two sharp-crested weir structures, both sets of data confirm the curves selected by Villemonte. In addition, the transition submergence was found to be zero for both structures. When both sets of data are plotted three-dimensionally, the rating curves shown in Figs. 17 and 18 are developed. The slope of the lines of constant submergence conform with the value of n_1 listed in Table 1 for the respective weirs.

Nappe Condition

During the tests conducted by the writers, consideration was given to the two types of nappe conditions which have been identified with submerged weirs: (1) the plunging nappe, and (2) the surface nappe. The Curved, dashed lines drawn in Figs. 12, 17, and 18 represent the dividing line between the two nappe conditions. The plunging nappe occurs for the lower values of submergence where the nappe plunges below the surface and remains there for a considerable distance from the weir before coming to the surface. At the point where the plunging nappe jet reaches the water surface, the surface velocity moves both upstream

towards the weir and downstream towards the outlet. The surface nappe condition occurs when the tailwater is raised sufficiently that the jet emanating from the constriction travels downstream on the water surface. Villemonte (1949) states that this type of nappe condition depends on the shape of the weir crest, submergence, and discharge.

These criteria were verified by the writers as shown in Figs. 12, 17, and 18. The curved dashed line drawn in each of these figures divides the plunging from the surface nappe condition. The plunging flow condition is to the right of the curve and the surface flow condition is to the left. Note that each curve is a function of discharge. The higher the discharge, the greater the value of submergence at which the nappe condition changes from plunging to surface.

When Crump (1952) analyzed the submerged flow data of Francis (1871) and Fteley and Stearns (1883), he found the nappe plunging under the surface at low submergence values as well as some negative submer-

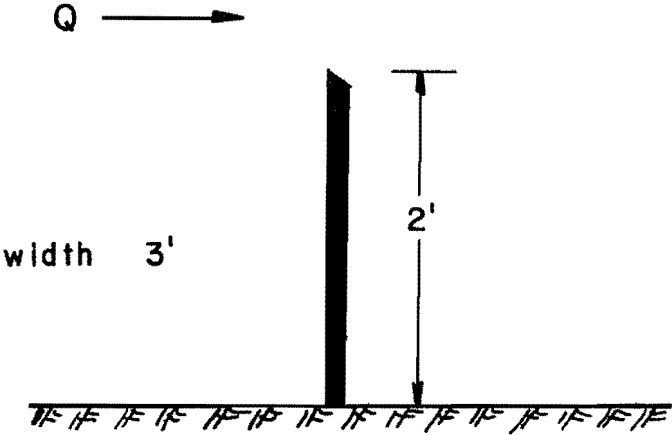


Fig. 13. Three-foot suppressed sharp-crested weir.

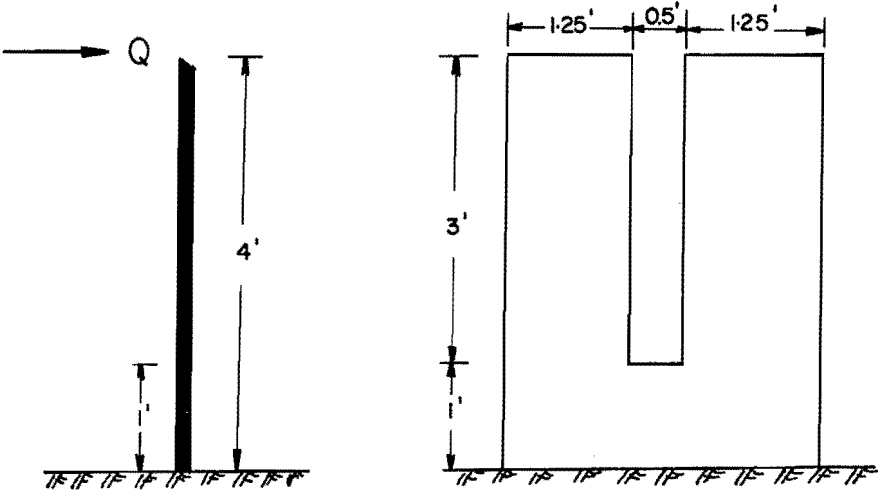


Fig. 14. Six-inch contracted sharp-crested weir.

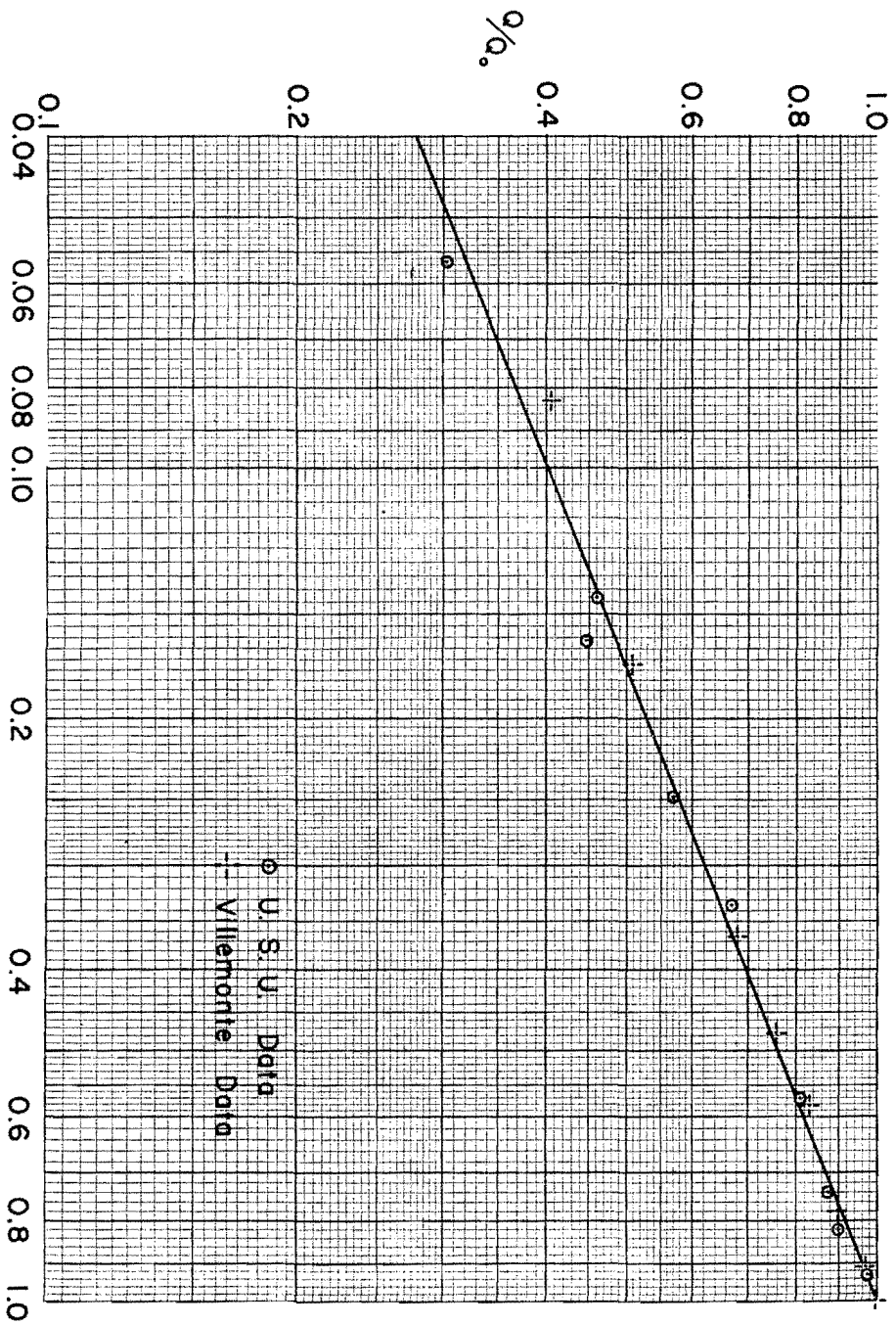


Fig. 15. Comparison of USU's and Villemonte's data for 3-foot suppressed sharp-crested weir.

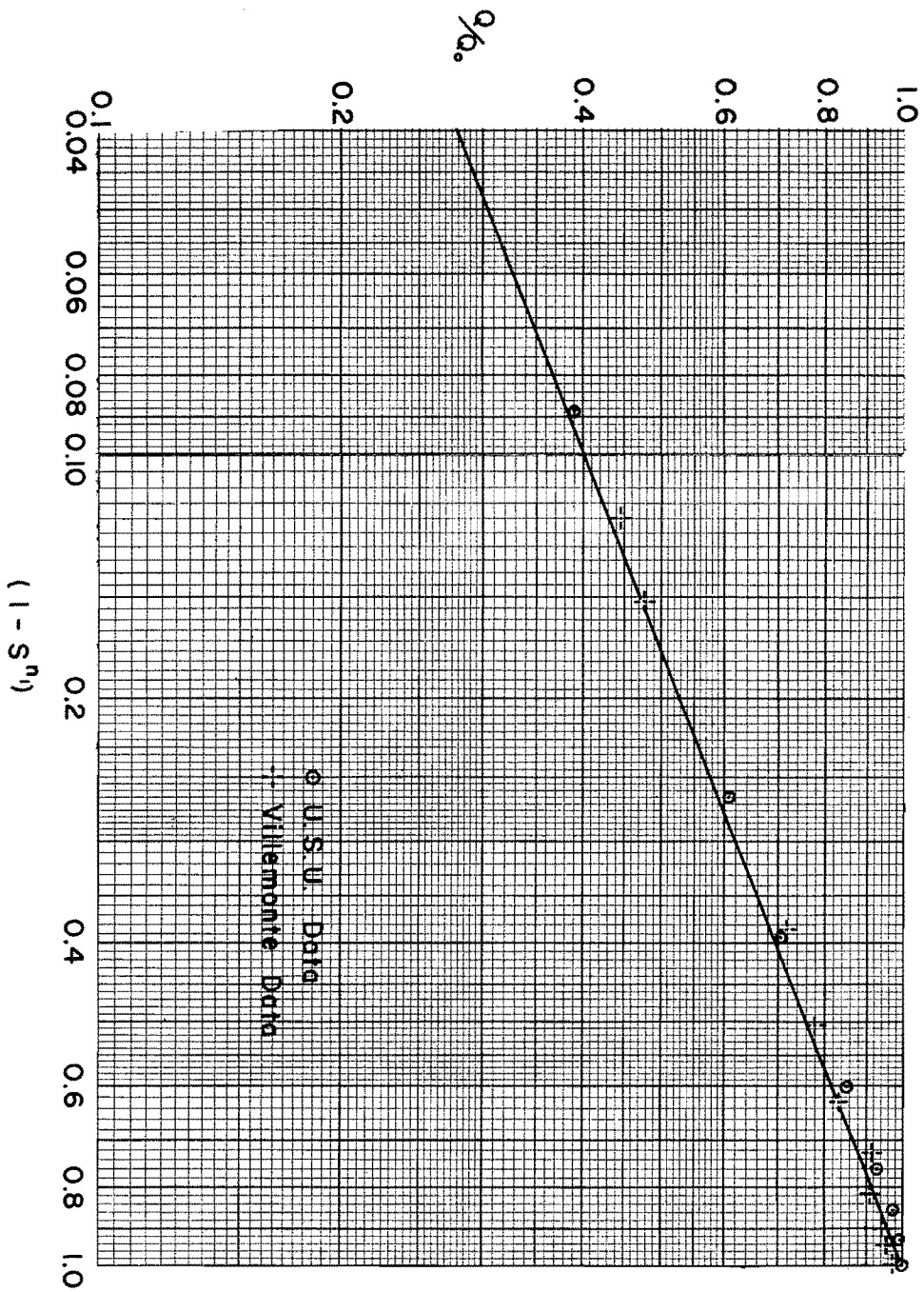


Fig. 16. Comparison of USU's and Villemonais's data for 6-inch contracted, sharp-crested weir.

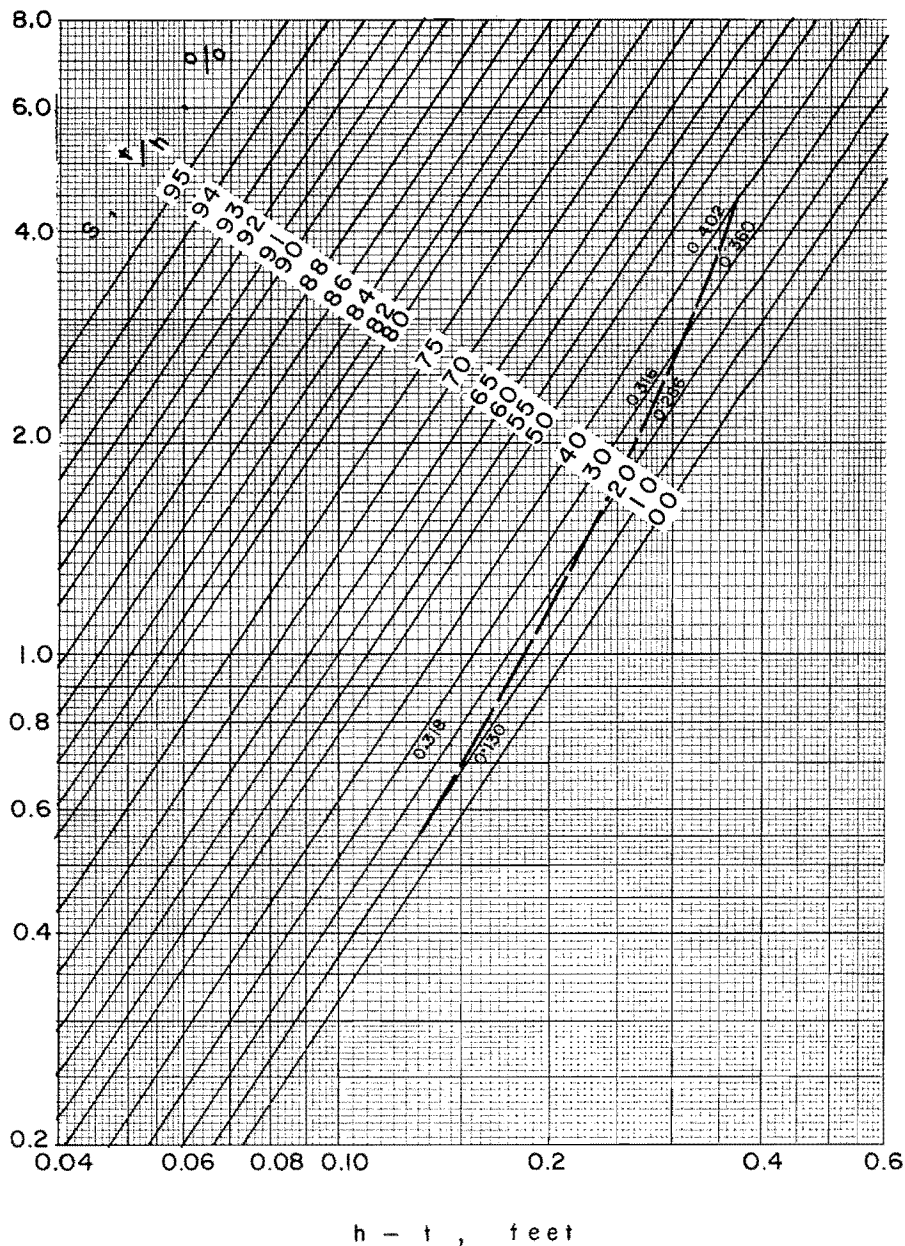


Fig. 17. Submerged flow calibration curves for 3-foot suppressed sharp-crested weir.

gence values. The weir crest was used as zero elevation datum. The explanation offered by Crump for his condition is that the transition submergence is reached well before the tailwater depth rises to the crest level. Before the transition point is reached, however, the nappe is discharging into free air and the air pocket is maintained at atmospheric pressure from the vents in the side walls. A mass of turbulent water is located below the air pocket. As the tailwater depth rises, the air pocket is replaced by water at less than atmospheric pressure, thereby increasing the curvature and velocities of the nappe at the control section. This actually carries a greater flow through the control section for the same given upstream

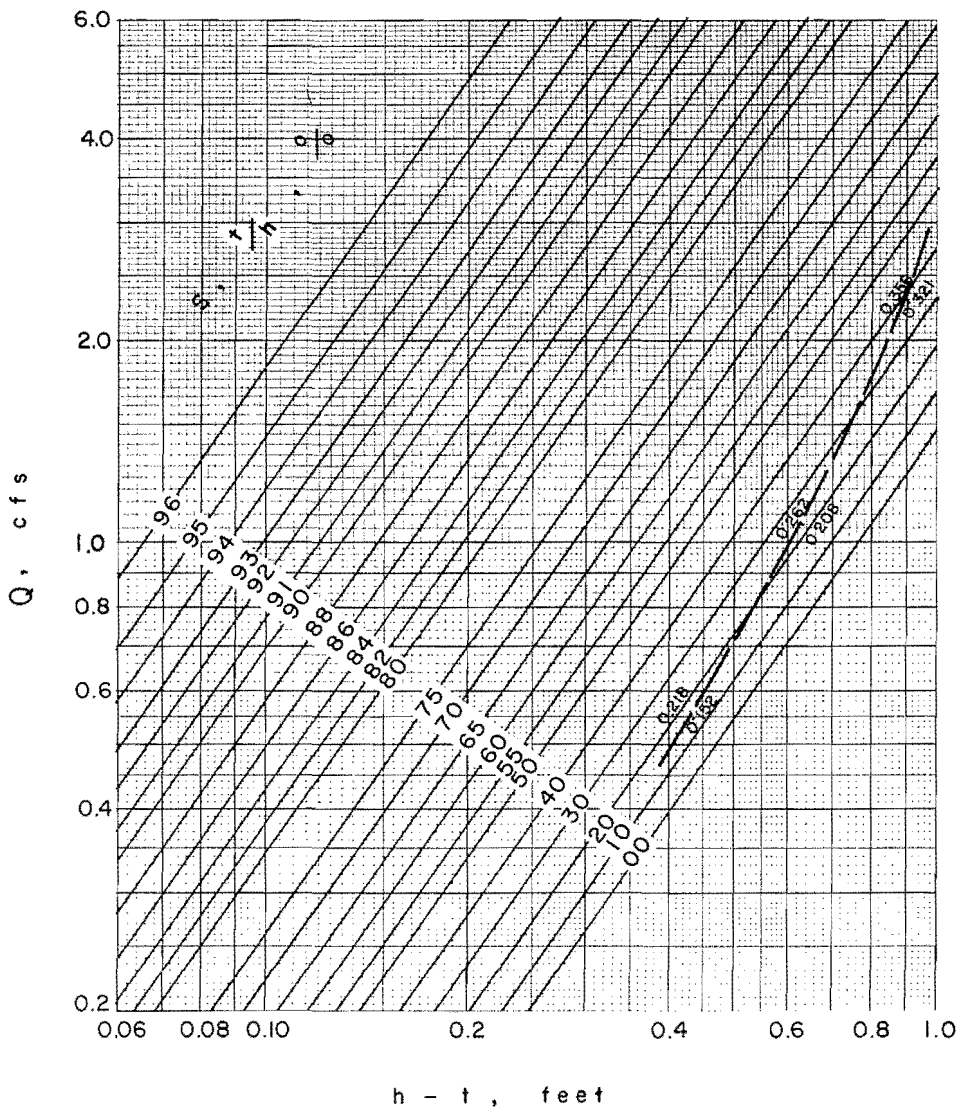


Fig. 18. Submerged flow calibration curves for 6-inch contracted sharp-crested weir.

depth. This condition exists until the degree of submergence rises, which increases the pressure on the under side of the nappe to the point where the air pocket is completely filled with water and drowns out the effect. Cox (1928) gives a similar explanation for the changing nappe conditions. He recommends that the submerged sharp-crested weir be operated with the nappe remaining on the surface, rather than plunging, if circumstances permit, for he found an overlapping of the two nappe conditions.

WEIR TYPES INVESTIGATED

The variety of weir types studied are listed in Table 1. The only weir of a broad-crested nature presented in this report is the highway embankment model studied by Kindsvater (1964). The embankment is discussed and illustrated in the sections where methods of analyzing submerged flow are developed (Figs. 1, 2, 3, 4, 5, 8, 10, and 11).

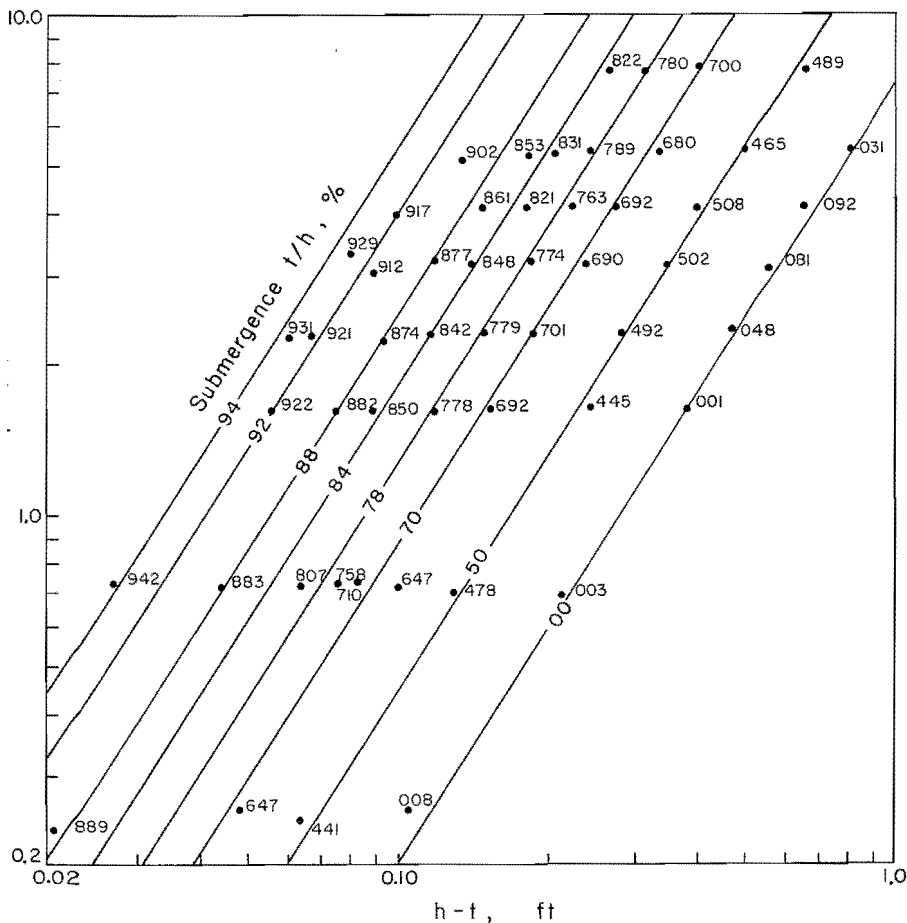


Fig. 19. Three-dimensional plot of submerged flow data for 2.00 foot high suppressed sharp-crested weir of Cox.

Suppressed Sharp-crested

Discussion and illustration of a 3-foot and 5-foot weir is given previously in this report. These weirs were tested to answer certain basic questions regarding submerged flow characteristics of weirs and to complement similar or identical studies conducted by other investigators. The three-dimensional submerged flow rating curves (Figs. 17 and 13) for the 3- and 5-foot suppressed sharp-crested weirs are shown in Figs. 17 and 13, respectively.

Cox (1928) investigated several sharp-crested weirs which ranged in height from 1.14 to 5.93 feet. Cox included in his report data collected on other sharp-crested weirs by Bazin (1888), Fteley and Stearns (1883), and Francis (1871). This submerged flow data was also analyzed utilizing the previously discussed concepts of submerged flow and found to verify the three-dimensional method of analysis, although the results have not

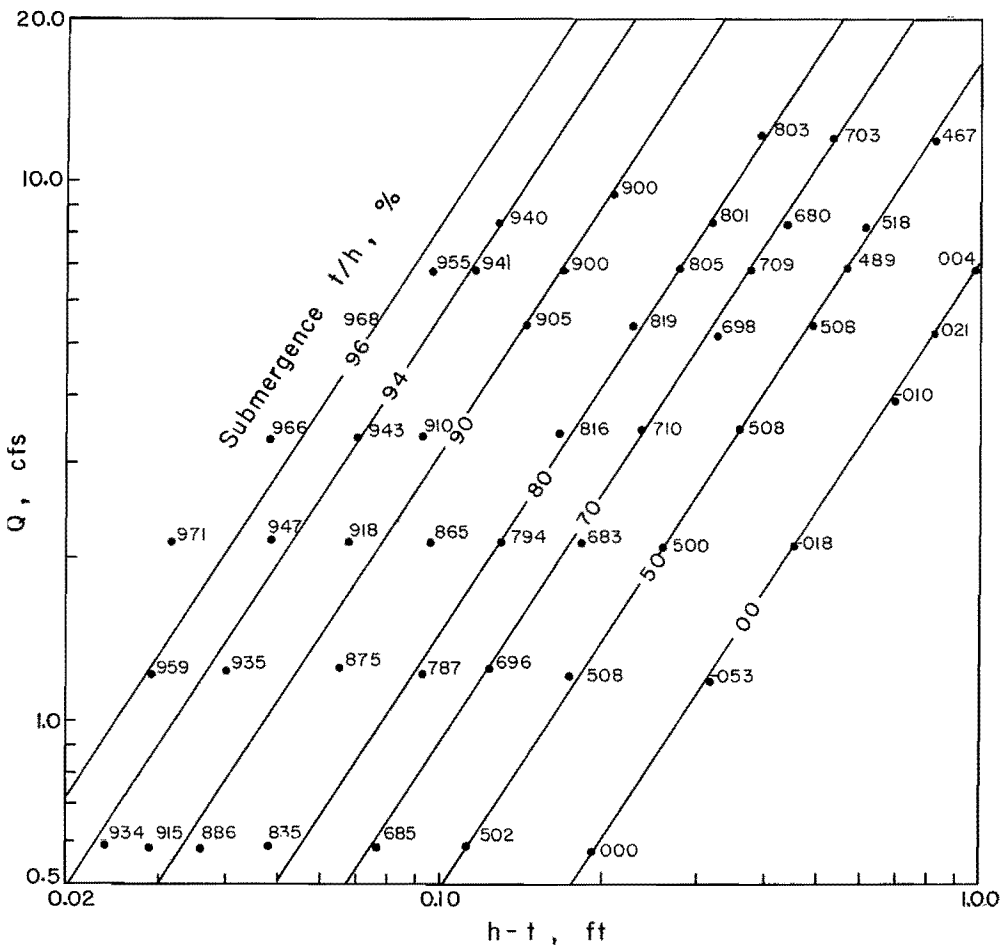


Fig. 20. Plot of submerged flow data for 5.93 foot high suppressed sharp-crested weir of Cox.

been included in this report because of the volume of material involved.

For purposes of illustration, only the data on the sharp-crested weirs of height 2.00 and 5.93 feet collected by Cox are subjected to the three-dimensional submerged flow analysis (Figs. 19 and 20). The lines of constant submergence were drawn to best fit the data using the slope resulting from the free flow calibration, which is 1.55 for the 2.00 foot high weir and 1.52 for the 5.93 foot high weir. The geometric properties

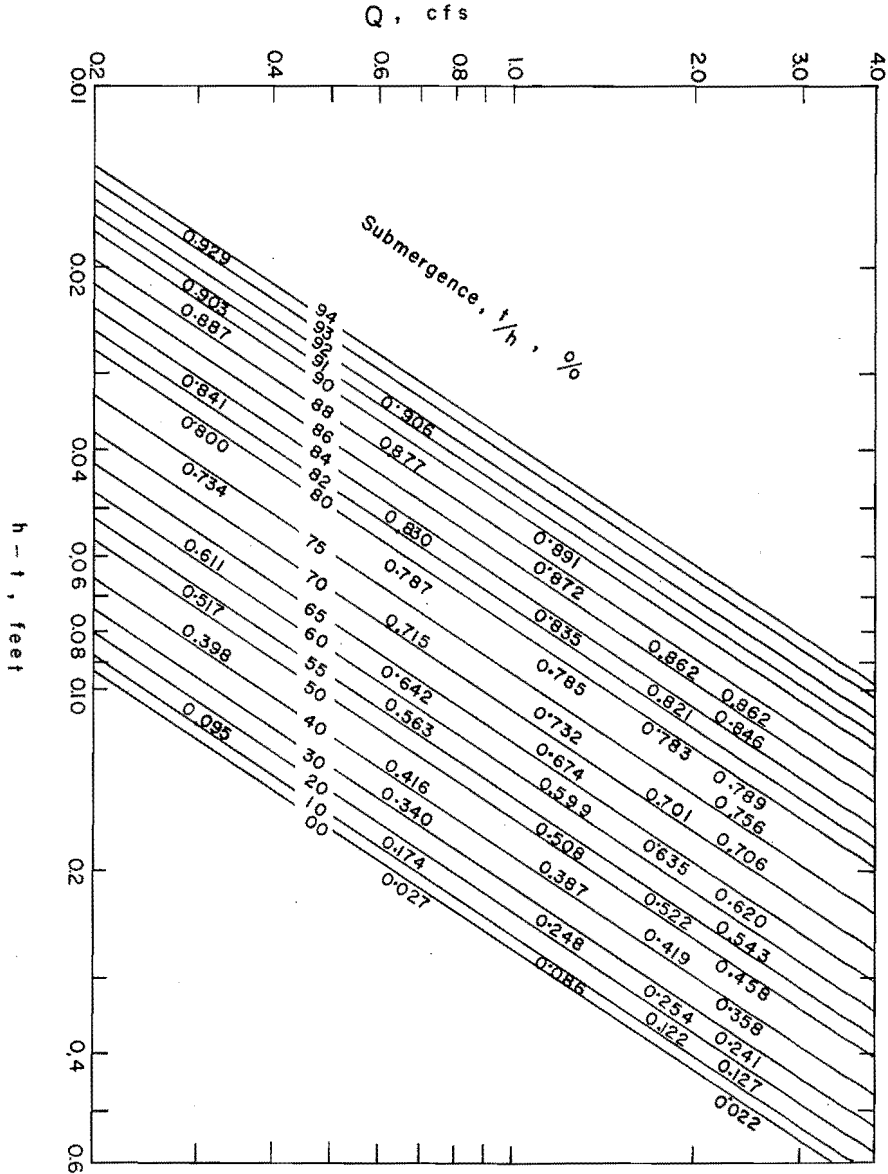


Fig. 21. Submerged flow calibration curves with data for 2-foot suppressed sharp-crested weir of Villemonste.

of the weirs are listed in Table 1, as are flow characteristics such as the transition submergence, and free and submerged flow equations. The submerged flow equations given for weirs having heights of 2.00 and 5.93 feet are limited in that they describe only the submerged flow regime from 50 to 96 percent, but do have merit because of their form (Eq. 1). Cox also investigated the relationship between weir height and the location for measurement of the tailwater or downstream flow depth. He states that the tailwater depth for sharp-crested weirs should be measured at a distance downstream from the weir of 2.54 times the weir height.

Another sharp-crested weir, tested by Villemonte (1949), is analyzed to lend additional verification to the three-dimensional submerged flow technique.

The information regarding the 2-foot suppressed sharp-crested weir is listed in Table 1. Analysis of the submerged flow data resulted in the submerged flow calibration curves shown in Fig. 21. These curves are drawn at a slope of 1.50.

Contracted Sharp-crested

Only one contracted sharp-crested weir is analyzed in this report. The 6-inch weir was investigated by Villemonte (1949) and the writers. The geometric properties and the flow characteristics of this weir structure are listed in Table 1. The three-dimensional submerged flow calibration curves for the 6-inch contracted sharp-crested weir are shown in Fig. 18.

Suppressed Ogee Crest

Koloseus (1951) conducted model studies on several ogee crest weirs to obtain design criteria for spillway and diversion dam structures. The submerged spillways, or weirs, had an ogee section which conformed to the profile of the lower nappe from a ventilated sharp-crested weir. The upstream face of the crest was vertical. A typical spillway structure studied by Koloseus is shown in Fig. 22.

The spillways studied had heights ($P + E$) from 0.5 to 2.0 feet with $h_d/(P + E)$ ratios varying from $1/4$ to 1 where h_d is the design head (depth). The testing was conducted in a flume with the spillway models

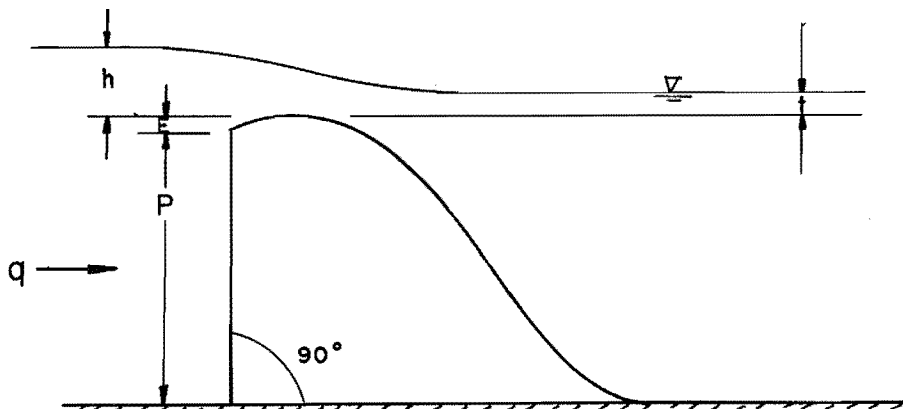


Fig. 22. Typical ogee crest weir studied by Koloseus.

placed 6.3 feet downstream from the flume entrance. Measurement of the flow depths, h and t , were made with a traversing point gage. The value used for the flow depths was taken as the average of three measurements taken downstream from the flume entrance, at distances of 1, 2, and 3 feet for the upstream depth of flow, and 14, 15, and 16 feet for the downstream depth of flow. To illustrate the submerged flow analysis, data was selected from the thesis of Koloseus (1951) for an ogee crest spillway having a height, $P + E$, of one foot and a $h/(P + E)$ ratio of $1/2$. The lines of constant submergence plot at a slope of 1.69 (Table 1). The three-dimensional plot of the data is shown in Fig. 23. Several lines of constant submergence are drawn, although not quite enough lines are present to classify the plot as a rating for the structure. A study of Koloseus' data indicates that the upstream depth of flow for any given discharge did not change until the downstream depth reached 50 to 60

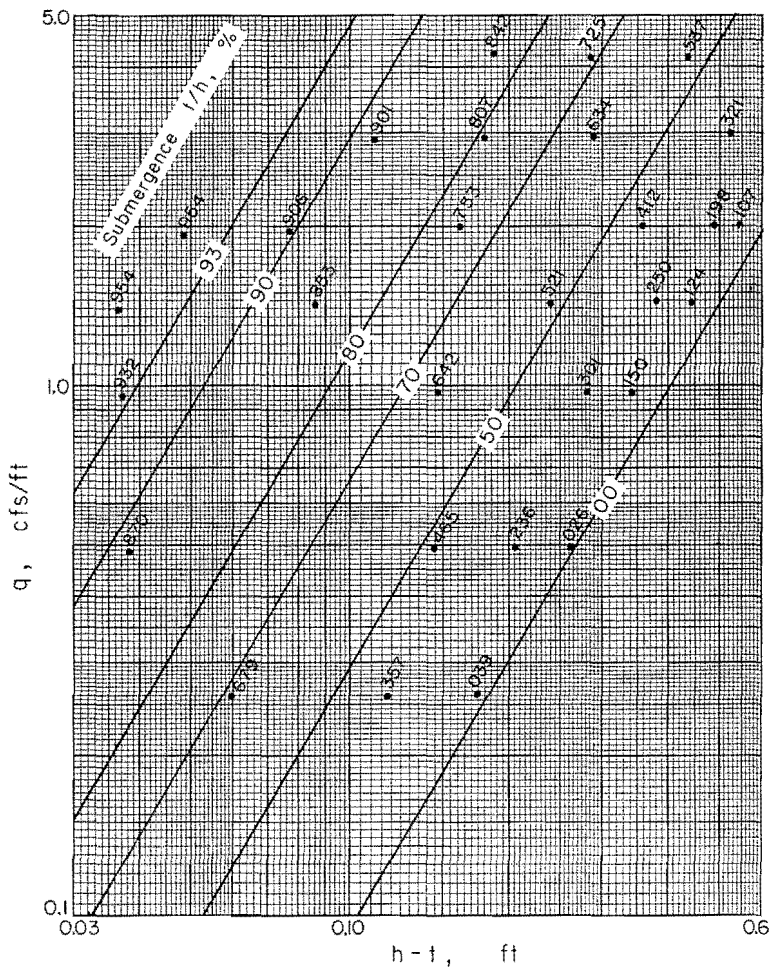


Fig. 23. Three-dimensional plot of submerged flow data for ogee crest weir studied by Koloseus.

percent of the upstream depth, using the spillway crest as a datum. Consequently, the transition submergence is roughly 50 or 60 percent. The approximate submerged flow equation written to fit the lines of constant submergence from 50 to 95 percent in Fig. 23 is

$$q = \frac{3.44 (h - t)^{1.69}}{[-(\log t/h + 0.0025)]^{1.20}} \dots \dots \dots (34)$$

Cox (1928) also conducted investigations with ogee crest weirs. The weirs varied in that some had a 2 to 1 upstream face, and others had a vertical face. The data from all six of the ogee crest weirs investigated by Cox have been analyzed by Hyatt, Skogerboe, and Austin (1966) to portray the validity of the three-dimensional submerged flow analysis. None of the ratings are shown in this report since the weir of Koloseus (1951) illustrates that ogee crest weirs are amenable to the three-dimensional submerged flow analysis.

The U. S. Bureau of Reclamation (1948) conducted model studies of submerged flow over overfall dams which were very similar in shape to those studied by Koloseus (1951). The data collected as part of the Boulder Canyon Project studies (U. S. Bureau of Reclamation, 1948) was subjected to the submerged flow rating analysis and found to be valid. The Bureau of Reclamation's study was limited in the range of discharge employed but the data did indicate that the analysis reported herein was applicable.

Crump Weir

The data collected by Crump (1952) for a weir having a triangular profile will be subjected to analysis. Fig. 24 shows the triangular weir-block which is referred to as a "Crump weir," named after its investigator. The width of the weir reported by Crump (1952) is 20 inches.

The submerged flow weir data from Crump's study (1952) is ideal for comparing the three submerged flow methods of analysis as previously described. The data is plotted in the manner used by Robinson (1964) in Fig. 25. Some scatter exists in the data making placement of the curve rather difficult. Nevertheless, the parameters which are plotted do show a very definite relationship exists. The value of submergence (transition submergence) for a Q/Q_0 ratio equal to one appears to be about 77 percent.

Crump's data is plotted in the manner proposed by Villemonte (1949) in Fig. 26. The variables bear a definite relationship to one another and the curve appears to fit the data reasonably well. However, the curve does not conform with the general curve advocated by Villemonte. This is because the transition submergence for the Crump weir is greater than zero percent. The transition submergence indicated in Fig. 26 is about 78 percent.

The three-dimensional plot of Crump's submerged flow data is shown in Fig. 27. The slope of the lines of constant submergence which best fit the data is 1.75, as given by the exponent, n_1 , in Table 1. Although the slope of 1.75 was selected for use in this analysis, some flexibility exists since only four free flow discharge values were available in developing the free flow rating.

In Fig. 27, several lines of constant submergence have been drawn at

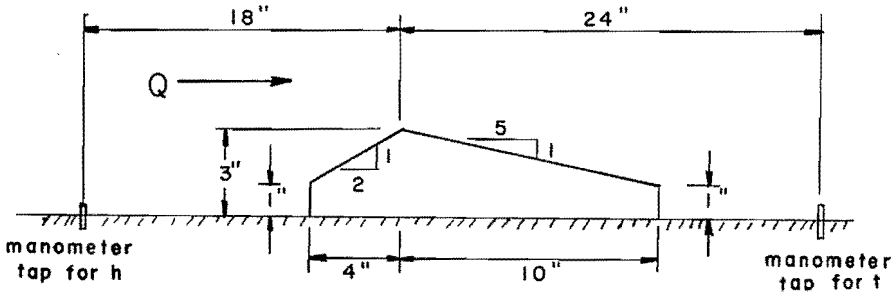


Fig. 24. Test model of Crump weir.

a slope of 1.75 which range in value from 75.0 to 97.7 percent. The submerged flow discharge equation written to describe this range is

$$Q = \frac{5.71 (h - t)^{1.75}}{[-(\log t/h)]^{1.36}} \dots \dots \dots (35)$$

By equating the free and submerged flow equations (Table 1) for the Crump weir, the transition submergence, S_t , can be obtained. The transition submergence obtained in this manner is 77 percent. This value of transition submergence has been drawn in Fig. 28 as the dividing line between free and submerged flow conditions. Justification for this is given by Crump (1952): "It is seen that the model has a high modular limit [transition submergence] of 70 percent, and that with a submergence ratio of 80 percent the departure from modularity [free flow] is less than 1 percent."

Hence, Fig. 28 can be used as the rating curves for either free flow or submerged flow conditions. The free flow discharge is obtained by entering the measured value of h from below and moving vertically upward until the 77 percent submergence line or free flow line is intersected and then moving horizontally to the left to obtain the discharge, Q . The submerged flow discharge is obtained by entering the measured $h - t$ value from above and moving vertically downward until the line of constant submergence t/h is intersected and then moving horizontally to the left, and reading the discharge value on the ordinate scale.

Other Weir Types

To provide additional verification, data from three other weir structures was subjected to the three-dimensional submerged flow analysis proposed by the writers. The weirs were selected because their shapes were different from any weirs previously discussed. The data was taken from the weir study by Villemonte (1949). The three weirs analyzed are (1) symmetrical proportional weir (Fig. 29), (2) 90° V-notch weir (Fig. 30), and (3) cusp parabolic weir (Fig. 31).

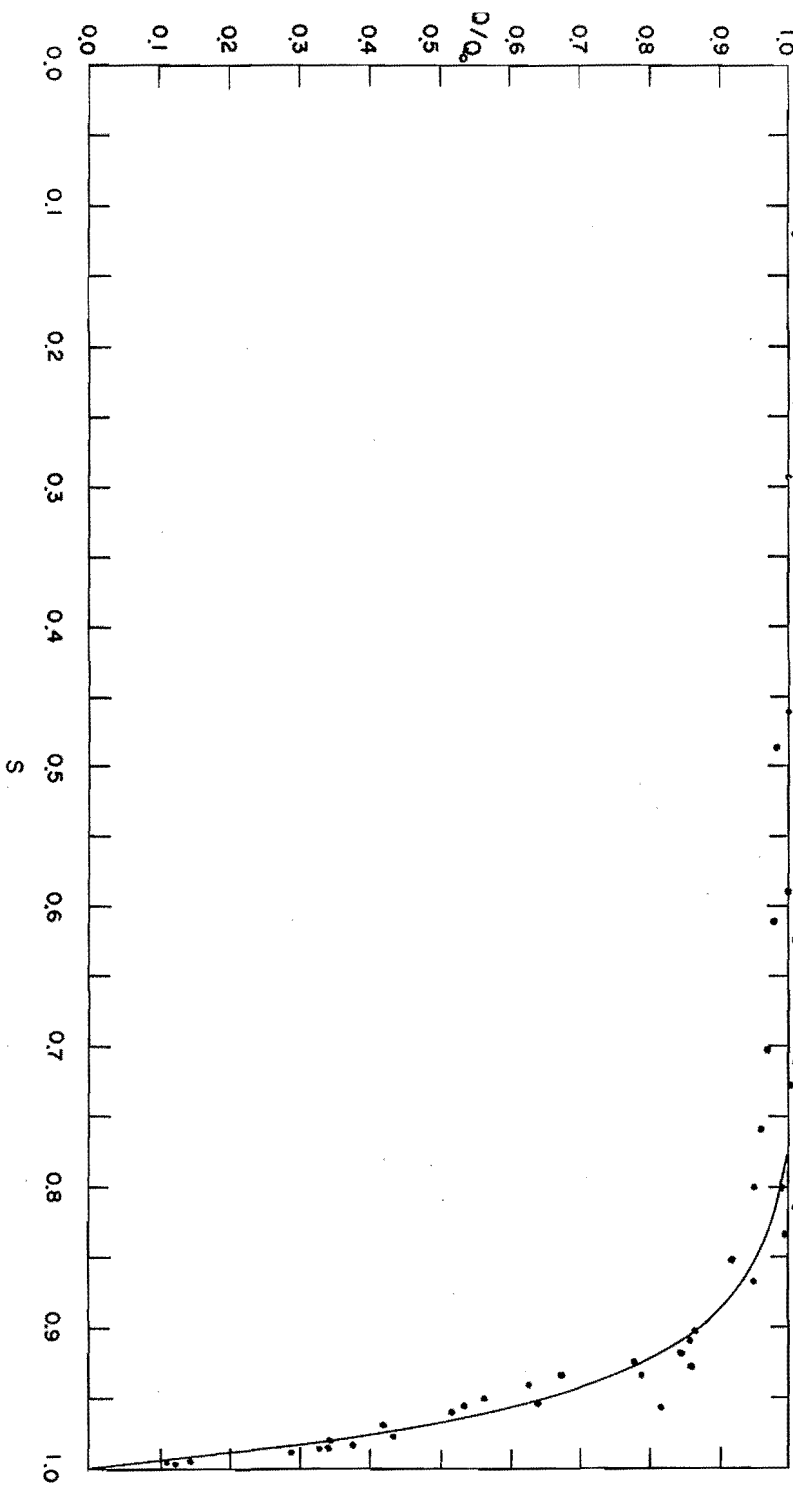


Fig. 25. Two-dimensional submerged flow plot of Crump weir data in manner used by Robinson.

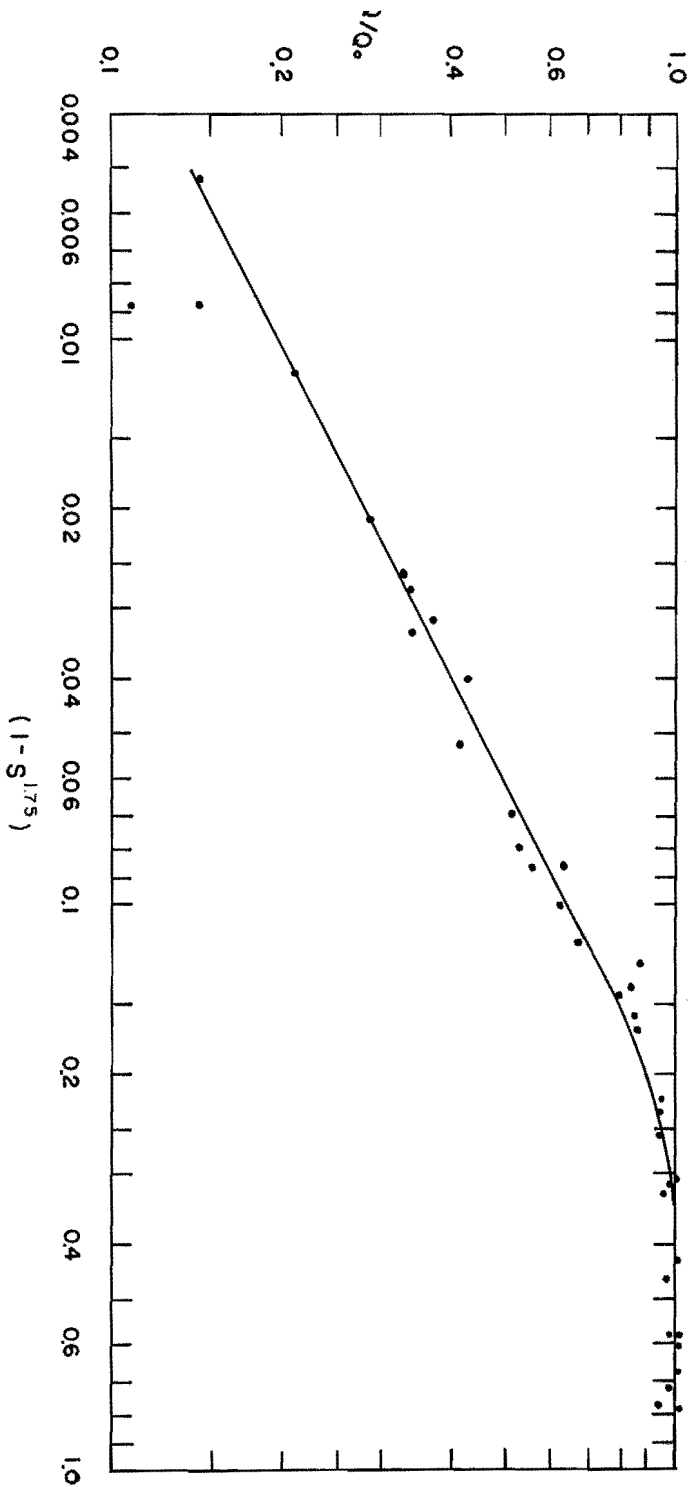


Fig. 26. Submerged flow plot of Crump weir data in manner proposed by Villemonte.

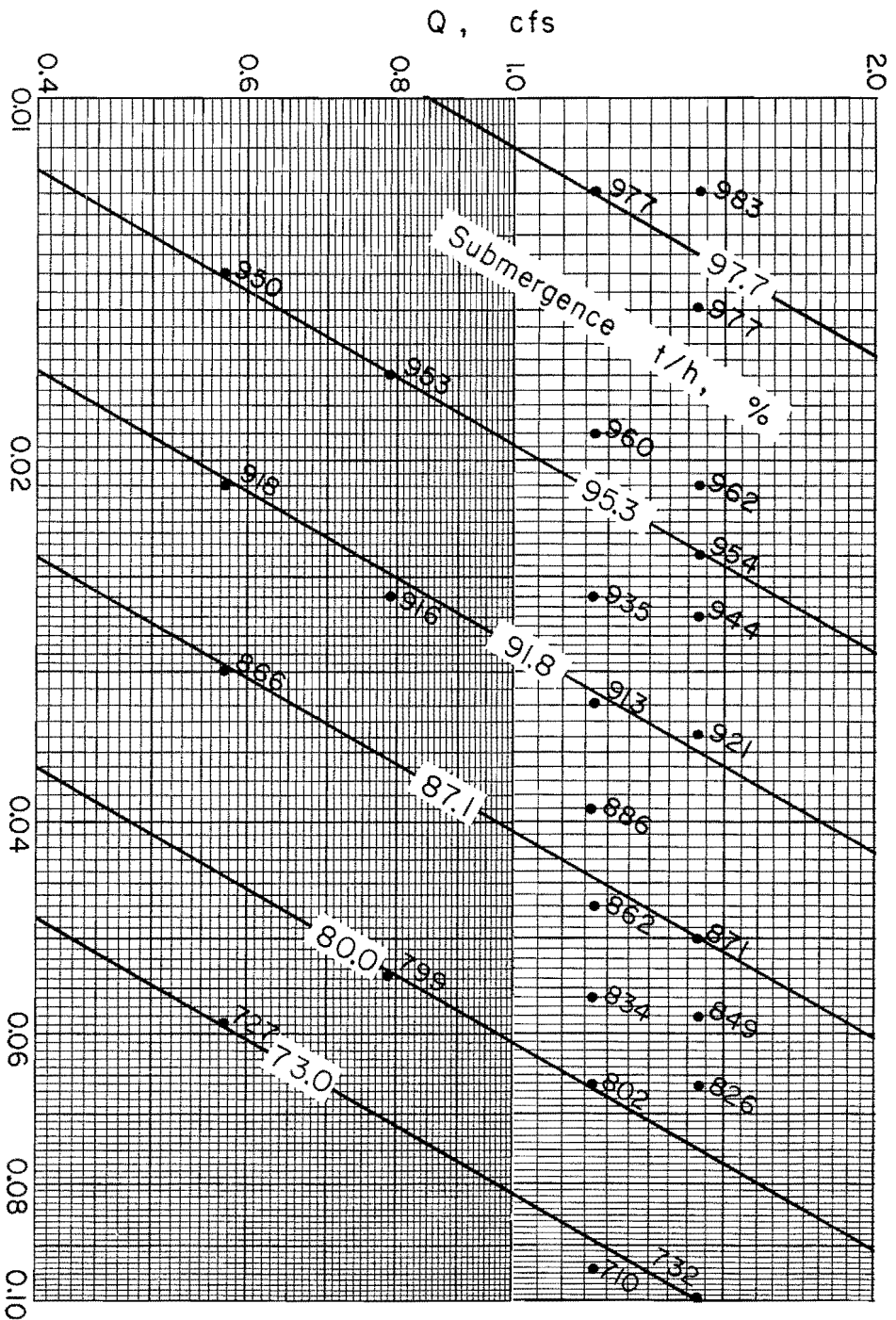


Fig. 27. Three-dimensional plot of submerged flow data for Crump weir.

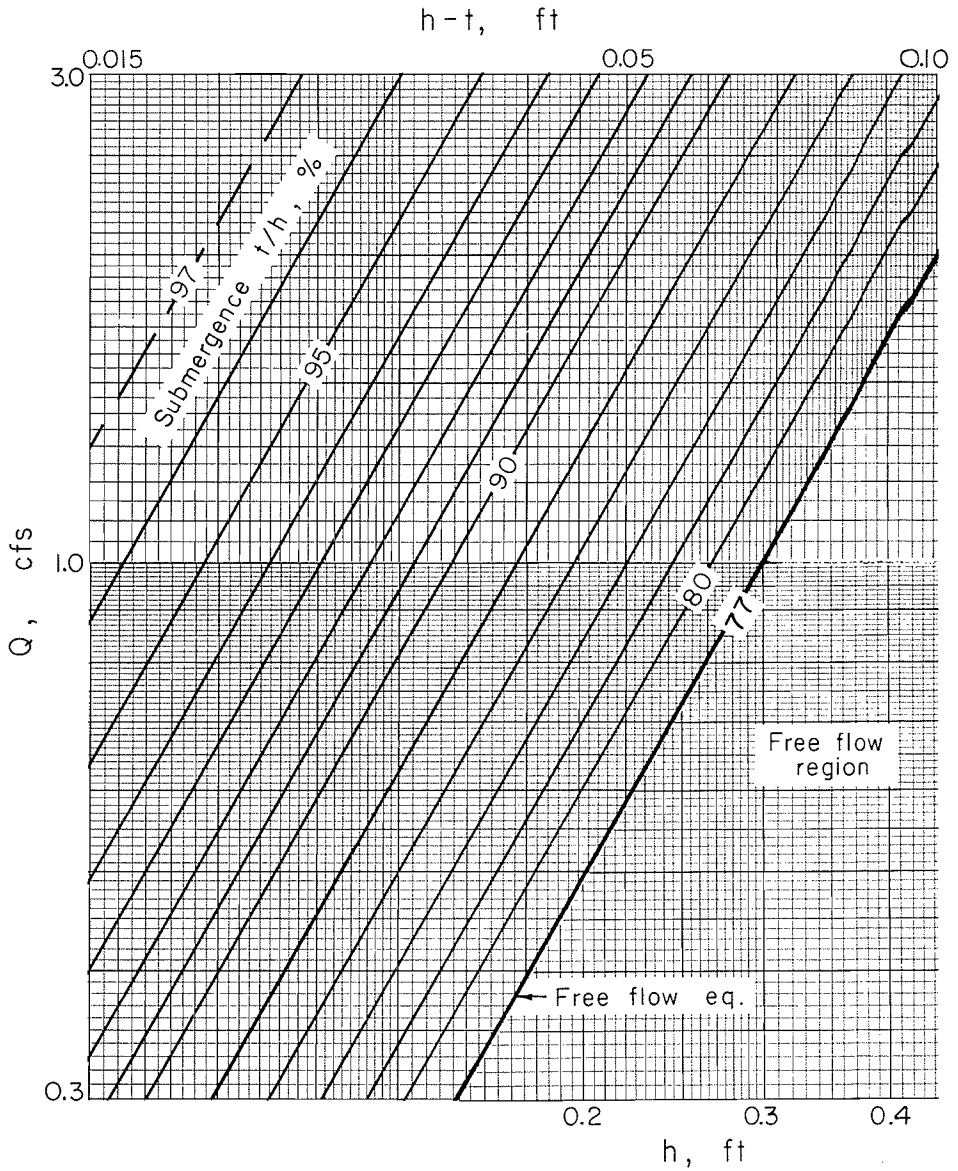


Fig. 28. Submerged flow and free flow calibration curves for Crump weir.

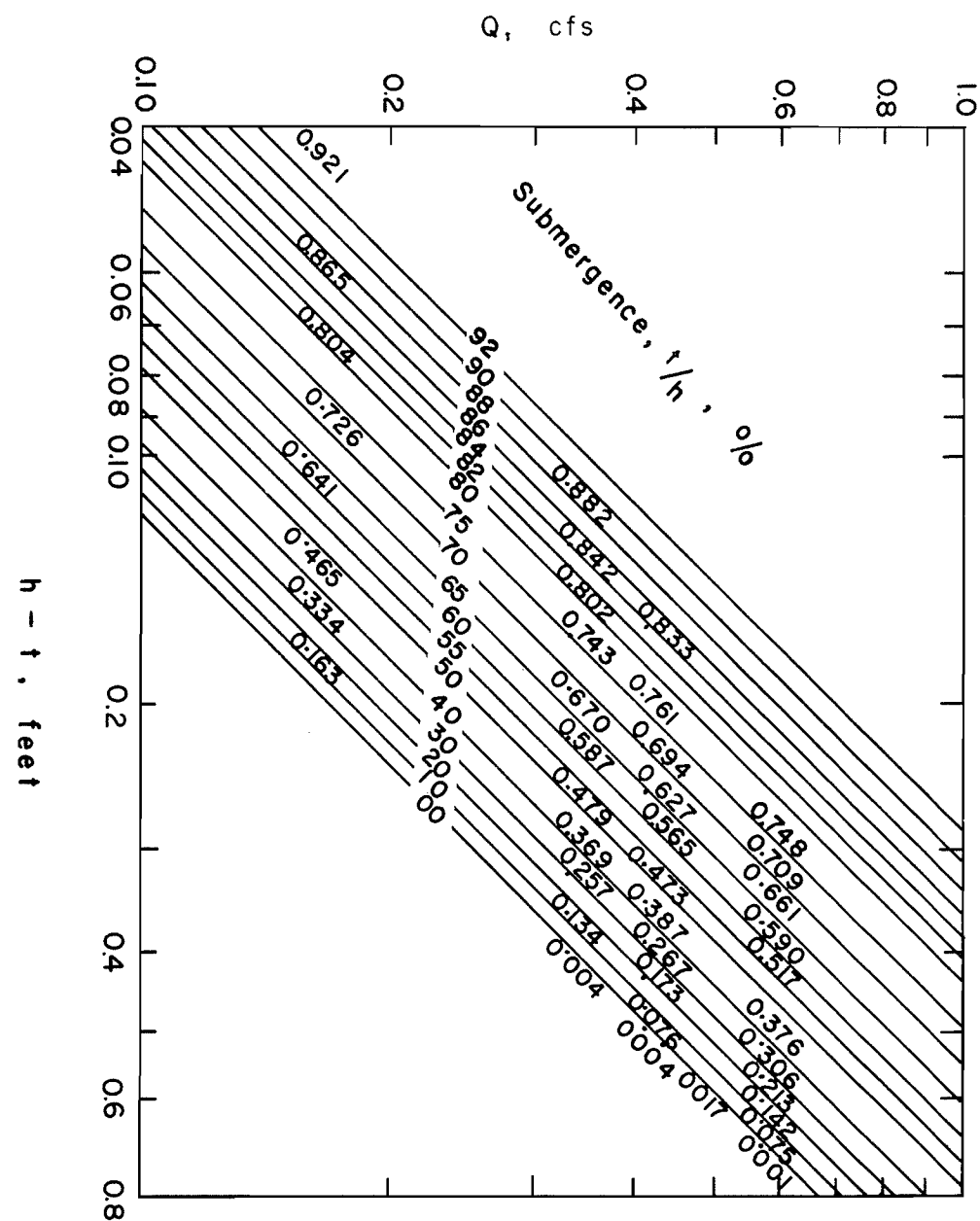


Fig. 29. Submerged flow calibration curves and plotted data for symmetrical proportional weir.

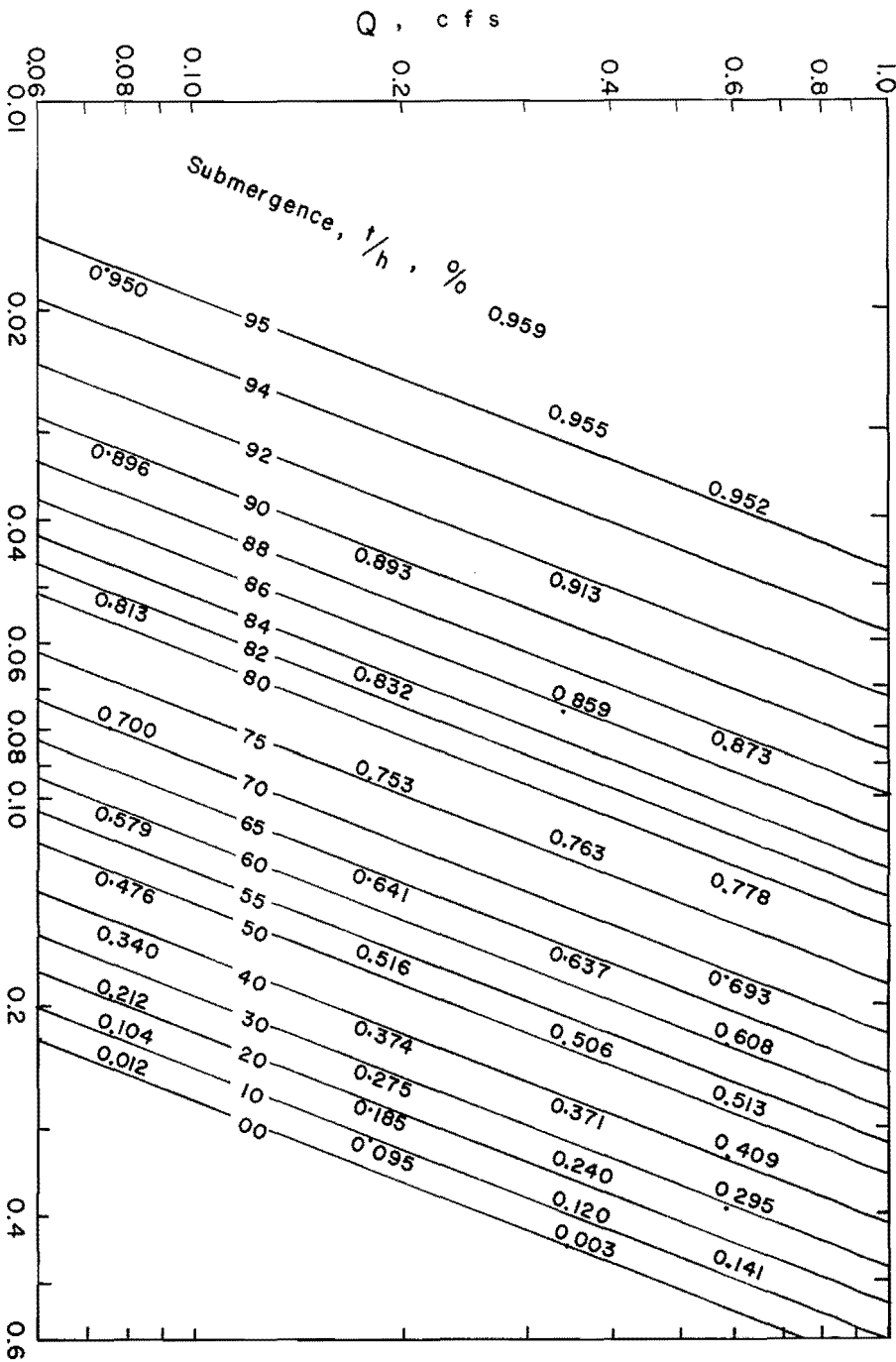


Fig. 30. Submerged flow calibration curves and plotted data for 90° V-notch weir.

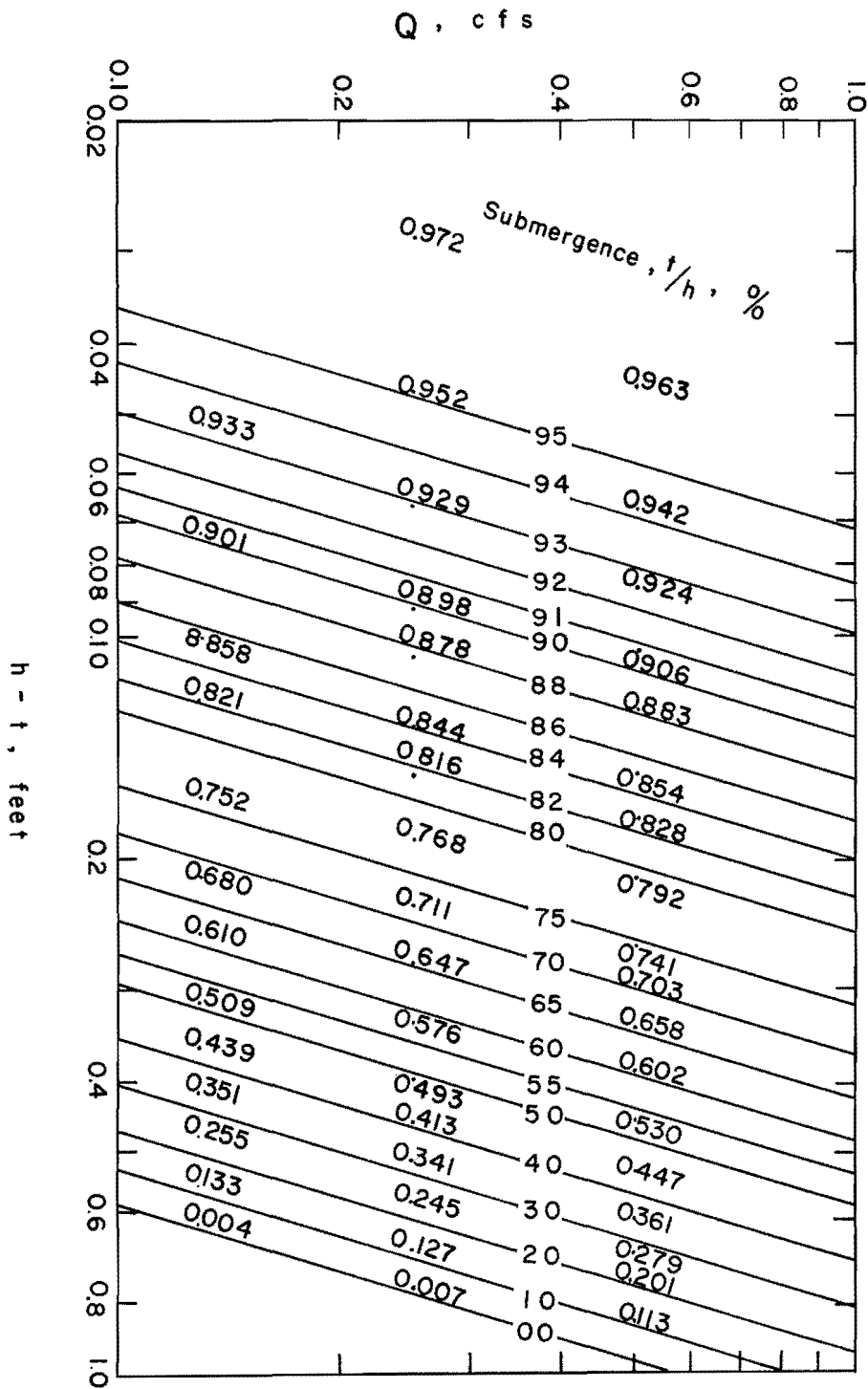


Fig. 31. Submerged flow calibration curves and plotted data for cusp parabolic weir.

SUMMARY

A number of methods for analyzing submerged (subcritical) flow over weirs have been developed by various investigators. Typical of the approaches applied to this particular problem are those reported by Robinson (1964) and Villemonte (1949). In addition, a method of analyzing submerged flow at open channel constrictions has been developed at Utah State University. All three methods of analysis have been compared by using data collected for various weir shapes. The comparisons showed each method of analysis to be correct, one method complementing each of the other methods. The primary advantage of the techniques developed at Utah State University is that the calibration curves are in reality the rating for any particular structure. The other methods do not yield discharge directly.

REFERENCES

- Bazin, H., 1888.** Experiences nouvelles sur l'écoulement en déversoir (Recent experiments on the flow of water over weirs), Mémoires et Documents, Annales des ponts et chaussées, 2e semestre. pp. 393-448, October. English translation by Arthur Marichal and John C. Trautwine, Jr., Proceedings, Engineers' Club of Philadelphia, 7(5):259-310, 1890; 9(3): 231-244 and (4): 287-319, 1892; and 10 (2): 121-164, 1893.
- Burgess, J. S., and W. R. White. 1966.** The triangular profile (Crump) weir — Two-dimensional study of discharge characteristics. Report No. INT 52. Hydraulics Research Station, Wallingford, Berkshire, England. May.
- Cox, Glen Nelson. 1928.** The submerged weir as a measuring device. Engineering Experiment Station, Series No. 67, University of Wisconsin, Madison, Wisconsin.
- Crump, Edwin Samuel. 1952.** A new method of gauging stream flow with little afflux by means of a submerged weir of triangular profile. Proceedings, Institution of Civil Engineers (London), Paper No. 5848, March, pp. 223-242. Discussions by G. Lacey, R. F. Wileman, J. H. Horner, E. Gresty, A. B. Tiffen, M. M. Kansot, and the author, No. 6, pp. 749-767, November.
- Doeringsfeld, H. A., and C. L. Barker. 1941.** Pressure — momentum theory applied to the broad-crested weir. Transactions, ASCE, 106: 934-969.
- Francis, J. B. 1871.** Experiments on the flow of water over submerged weirs. Transactions, ASCE, 13: 303. (As reported by Cox.)
- Fteley, A., and F. P. Stearns. 1883.** Description of some experiments on the flow of water made during the construction of works for conveying the water of Sudbury River to Boston. Transactions, ASCE, 12: 101. (As reported by Cox.)
- Hyatt, M. Leon. 1965.** Design, calibration, and evaluation of a trapezoidal measuring flume by model study. MS Thesis, Utah State University, Logan, Utah. March.
- Hyatt, M. L., G. V. Skogerboe, and L. H. Austin. 1966.** Subcritical flow over various weir shapes. Report WR6-8, Utah Water Research Laboratory, College of Engineering, Utah State University, Logan, Utah. June.

Kindsvater, Carl E. 1964. Discharge characteristics of embankment-shaped weirs. Geological Survey Water-Supply Paper 1617-A. U. S. Geological Survey and Georgia Institute of Technology.

Koloseus, Herman J. 1951. Discharge characteristics of submerged spillways. MS Thesis, Colorado Agricultural and Mechanical College, Fort Collins, Colorado. December.

Robinson, A. R. 1964. Water measurement in small irrigation channels using trapezoidal flumes. Paper No. 64-210, presented at 1964 annual meeting of ASAE. Fort Collins, Colorado. June.

Skogerboe, G. V., M. L. Hyatt, and L. H. Austin. 1966. Stage-fall-discharge relations for flood flows over highway embankments. Report WR6-7, Utah Water Research Laboratory, College of Engineering, Utah State University, Logan, Utah. March.

Skogerboe, G. V., M. L. Hyatt, and K. O. Eggleston. 1967. Design and calibration of submerged open channel flow measurement structures: Part 1, Submerged flow. Report WG31-2, Utah Water Research Laboratory, College of Engineering, Utah State University, Logan, Utah. February.

Skogerboe, G. V., M. L. Hyatt, J. R. Johnson, and J. D. England, 1965. Submerged Parshall flumes of small size. Report WR6-1, Utah Water Research Laboratory, College of Engineering, Utah State University, Logan, Utah. July.

Skogerboe, G. V., W. R. Walker, and L. R. Robinson. 1965. Design, operation, and calibration of the canal A submerged rectangular measuring flume. Report WG24-3, Utah Water Research Laboratory, College of Engineering, Utah State University, Logan, Utah. March.

U. S. Bureau of Reclamation. 1948. Studies of crests for overfall dams. Boulder Canyon Project Final Reports, Part 6 — Hydraulic Investigations, Bulletin 3, U. S. Department of the Interior.

Villemonste, James R. 1949. Effect of submergence on discharge of sharp-crested weirs. PhD Dissertation, University of Wisconsin, Madison, Wisconsin.

Yarnell, D. L., and F. A. Nagler. 1930. Flow of flood water over railway and highway embankments. Public Roads, 11: 30-34. April.